

# CHAOTIC SCATTERING BY STEEP POTENTIALS

A.RAPOPORT AND V. ROM-KEDAR

ABSTRACT. The singular billiard limit of smooth steep scattering potentials is utilized as a skeleton for studying the properties of the scattering problem; It is shown that for one class of chaotic scatterers, named here regular Sinai scatterers, the scattering properties of the smooth system limit to those of the billiard. On the other hand, it is shown that for other chaotic scatterers, that belong to the class of singular Sinai scatterers (scatterers with singular bounded semi-orbits), the fractal dimension of the scattering function of the smooth flow may be controlled, for arbitrary steep potentials, by changing the ratio between the steepness parameter and a parameter which controls the billiards' geometry.

## 1. INTRODUCTION

When a ray of inertial trajectories, parameterized by an input parameter, enters an interaction region in which the trajectories are modified by nonlinear forces, the ray is scattered and leaves the region in different directions. The common characteristics observed upon leaving the interaction region are the *escape angle* and the *residence time*. These are called *scattering functions* of the input parameter. Scattering problems arise in a wide spectrum of models in physics and chemistry (see [29] and [30]): celestial mechanics [17, 31, 5, 18], charged particle trajectories in electric and magnetic field [8, 6], hydrodynamical processes [28, 1, 37], models of chemical reactions [32, 27, 14, 24] and scattering in atomic and nuclear physics [46, 47]. Typically, most of the trajectories stay in the interaction region for a finite time. However, in an open Hamiltonian system there may exist a Lebesgue-measure-zero set of input parameters producing trajectories that are trapped in the interaction region for an arbitrary long time. This measure-zero set gives rise to strong oscillations in the scattering functions, influencing the nearby trajectories. If this set of singularities of the scattering function,  $I$ , has a positive fractal dimension<sup>1</sup>, then the scattering is called chaotic, otherwise it is called regular.

First, it was noticed that when the invariant set associated with the scatterers has chaotic components, the singularity set  $I$  of trapped trajectories, which includes all initial conditions belonging to the stable manifold of the chaotic invariant set, is fractal [13, 19]. Subsequently, the structure of  $I$  was examined in diverse scattering problems. Hard wall scatterers were studied in several two-dimensional geometries (three hard discs scatterers [13, 14], three hard discs and a uniform magnetic field [6], billiard traps with two openings [2, 36] and a wedged billiard with gravity [16, 5]). Most of these two-dimensional billiard models were constructed so that the invariant set in the interaction region may be fully characterized using symbolic dynamics, and thus particle escape rates and other scattering characteristics may be found using the thermodynamic formalism [14][12].

Scattering by finite range axis-symmetric potential hills and by smooth potential hills were studied in [19, 3, 42, 4, 11, 29, 6, 15] whereas scattering by smooth attractive potential wells were studied in [9, 10]. In many of these works it was noted that bifurcations leading

---

<sup>1</sup>usually one uses the box-counting or the uncertainty dimension [3, 4, 25].

to structural changes in the invariant set change the fractal dimension of the scattering functions. In [20] a unified framework for studying scattering in several smooth classical and quantum systems is presented. In [21][22][23] scattering by sums of  $n$  attractive or  $n$  repelling Coulombic potentials were studied in the high energy limit, where it was proved that for generic placement of the centers the (chaotic for  $n \geq 3$ ) scattering is hyperbolic and its properties are universal, depending only on  $n$ , and can thus be explicitly analyzed. In the more general smooth case (or for low energy values in the Coulombic case), one cannot predict what would be the dependence of the invariant set on various parameters - the phase space structure of such two-degrees of freedom non-integrable systems is usually too complex: it admits mixed dynamical regimes, and numerous types of local and global bifurcations. Three such bifurcations were previously discussed in the context of chaotic scattering by smooth potentials - the local saddle-center and period doubling bifurcations [4, 11][25], and the global abrupt bifurcation [3]. It was noted that the appearance of islands of stability via these local bifurcations leads to a scattering functions with fractal dimension one [4, 11][25]. On the other hand, it was noted that the abrupt bifurcation, by which lowering the energy below a critical energy value  $E_c$  leads to a sudden change in the topology of the Hill's region (the region of allowed motion in the configuration space [26]), creates, for circularly symmetric hills [3, 4] and for non-circular (elliptic) hills [4, 41], a hyperbolic invariant set which is structurally stable, named *fully developed chaotic scattering* [3]. At the critical value of the energy the energy surface contains a saddle point and its separatrices, so the appearance of abrupt bifurcations may be related to the study of the generic (or symmetric) homoclinic bifurcations associated with such structures [45, 39].

Summarizing, from the above studies the following classification of scattering problems emerges; when the invariant set is simple (consists of a countable number of unstable periodic orbits) *regular* scattering is produced and the fractal dimension of  $I$  vanishes. When the invariant set is hyperbolic and has a positive fractal dimension, *hyperbolic chaotic* scattering is created and the fractal dimension of  $I$  is larger than zero and less than one. Finally, when the invariant set, is *non-hyperbolic* and contains KAM-tori (so it has positive Lebesgue measure), *non-hyperbolic chaotic* scattering is observed and the fractal dimension of  $I$  appears to be close to 1. While for many billiard problems and finite range potentials the invariant set may be explicitly constructed by geometrical means, for the smooth case its structure is complex and is usually found via numerical simulations.

Here, we present a class of smooth<sup>2</sup> non-trivial scattering problems that can be rigorously analyzed; We consider the scattering of a ray of particles by a family of smooth scattering steep potential  $W(q; \varepsilon)$ , which, in the limit  $\varepsilon \rightarrow 0$ , becomes the hard-wall billiard scatterer  $D = \cup_{i=1}^N D_i$  :

$$(1) \quad H = \frac{\|p\|^2}{2} + W(q; \varepsilon).$$

$$(2) \quad W(q; \varepsilon) \xrightarrow{\varepsilon \rightarrow 0} \begin{cases} 0 & q \in \mathbb{R}^2 \setminus D \\ E_i & q \in \partial D_i. \end{cases}$$

Here  $D_i$  are compact closed domains called obstacles (of "height"  $E_i$ , where  $E_i > 0$  and may be infinite),  $N$  is finite, and  $D$  is compact as well, namely the distance between the obstacles is bounded. Following [43], the billiard-like potential family  $W(q; \varepsilon)$  is assumed to satisfy some natural conditions that are specified for completeness in the appendix. One may

<sup>2</sup>Hereafter, smooth means  $C^{r+1}$  potentials with  $r$  sufficiently large for KAM theory to apply near stable orbits (so, we take  $r > 3$ . In the examples  $r = \infty$ ).

simply think of  $W$  as the sum of potentials  $V_i(z)$  that decay sufficiently rapidly with  $z$  (e.g. exponentials, Gaussians or power-law potentials) depending on  $z = Q_i(q)/\varepsilon$ , where  $Q_i(q)$  denotes the signed smooth distance function (so  $Q_i(q)|_{q \in \mathbb{R}^2 \setminus D_i} > 0$  and  $Q_i(q)|_{q \in D_i} \leq 0$ ) e.g.:

$$(3) \quad W(q; \varepsilon) = \sum_{i=1}^N \mathcal{E}_i \exp\left(-\frac{Q_i(q)}{\varepsilon}\right).$$

where  $\mathcal{E}_i$  represents here the strength of the  $i$ th obstacle which is of infinite height, or

$$(4) \quad W(q; \varepsilon) = \sum_{i=1}^N E_i \exp\left(-\frac{Q_i(q)^2}{\varepsilon}\right).$$

where  $E_i$  represents here the height of the  $i$ th obstacle. Let

$$\mathcal{E} = \inf_i \{\mathcal{E}_i, E_i\}.$$

Our analysis applies to intermediate energy levels  $h$ :

$$0 < h < \mathcal{E}.$$

For such energy levels, for sufficiently small  $\varepsilon$  values, the particle moves essentially freely between the obstacles and bounces off their boundary when it encounters them. In the terminology of [3] we are always concerned here with energies below the critical energy of the abrupt bifurcation, namely we do not consider here effects that are associated with topological changes in the Hill's region. Intuitively, one would suspect that for such energy levels and small  $\varepsilon$  values, the scattering by the billiard scatterers and by the smooth flow will be very similar (see [3]). Using the recently developed analytical methods of [43, 38, 44, 34, 33, 35], in which similarities and differences between  $n$ -dimensional ( $n \geq 2$ ) smooth Hamiltonian flows with steep billiard like potentials and billiards flows were studied, we show that the billiard limit is useful for analyzing the smooth behavior, yet their scattering profiles may be substantially different.

Another issue which naturally arises from our analysis is the study of singularities in the dynamics of the billiard scatterers and their influence on the scattering function. While tangent singularities had appeared naturally in the dispersing scatterers context [13, 14][42], the corner singularities, that arise when the scatterer boundary has corners, have been essentially neglected (though see [16, 5]). We thus dedicated part of this paper to demonstrate the influence of corners on the scattering function. The presented findings for this case are preliminary and are of great interest: these results show how the smoothness properties of a spec of dust may influence the scattering from a nearby large obstacle.

The paper is ordered as follows: in Section 2 we present the set up for the billiard scattering problem, define regular and singular Sinai scatterers, and explain how tangencies and corners influence their invariant set and the scattering functions. To demonstrate these effects we introduce two families of singular Sinai billiard scatterers. In section 3 a paradigm for studying chaotic scattering by smooth steep billiard-like potentials is presented. There, we conclude that for regular Sinai scatterers the steep smooth flow and the limiting billiard scatterer have similar chaotic scattering functions. Then, in Section 4, the scattering by steep smooth potentials is investigated when the limiting billiards are singular, having either a corner polygon or a tangent periodic orbit. Based upon the obtained numerical results and the findings in [43, 38, 44, 34, 33, 35], it is demonstrated that the fractal dimension of the scattering function of the steep smooth potential can be controlled in such cases. In the appendix we include precise statements regarding the classes of potentials we consider and the rigorous statements that apply to these.

## 2. BILLIARD SCATTERING

**2.1. Formulation:** Consider a scattering billiard in  $\mathbb{R}^2$ ; Let  $S_R \subset \mathbb{R}^2$  denote a circle, centered at the origin, of finite radius  $R$ , parameterized by  $s \in [0, 2\pi)$  (with  $s = 0$  corresponding to the direction of the positive  $x$  axis). The scatterer  $D$ , a collection of hard wall obstacles, reside inside  $S_R$ . The obstacles are assumed to have piecewise smooth,  $C^{r+1}$  components ( $r > 3$ ). We call the scatterer  $D$  a *Sinai scatterer* if its boundary is composed of a finite number  $\bar{n}$  of  $C^{r+1}$ -smooth *scattering* components  $\Gamma_i$  that are either bounded away from each other by some minimal distance or have pairwise intersections at angles that are bounded away from zero (no cusps are allowed). We denote by  $\Gamma^*$  the corner set at which the scatterer boundary is not smooth. Some of our results apply to a general scatterer geometry, yet, we will mostly consider Sinai scatterers.

A typical trajectory enters  $S_R$  at some  $s_{in}$  with velocity  $(p_x, p_y) = \sqrt{2h}(\cos \varphi_{in}, \sin \varphi_{in})$ , moves freely under the billiard flow, reflecting elastically from the obstacles inside  $S_R$ , until it exits  $S_R$ , at time  $t_{out}$ , at some point  $s_{out}$  with velocity in the direction  $\varphi_{out}$ . Thus, the  $R$  dependent scattering map:

$$(5) \quad \mathcal{S}(R) : (s_{in}, \varphi_{in}) \rightarrow (s_{out}, \varphi_{out}, t_{out})$$

may be naturally defined. Instead of using the  $R$ -dependent coordinates  $s_{in}, s_{out}$  it is traditional to define the  $R$ -independent impact parameters  $b_{in}$  and  $b_{out}$ :

$$(6) \quad b_{in} = R \sin(\varphi_{in} - s_{in}) \quad \text{and} \quad b_{out} = R \sin(\varphi_{out} - s_{out}).$$

The scattering time  $t_{out}$  dependence on  $R$  can then be explicitly defined as:

$$(7) \quad t_{out}(b_{in}, \varphi_{in}; R, h) = \frac{\mathcal{L}(b_{in}, \varphi_{in}; R)}{\sqrt{2h}}$$

$$(8) \quad = \frac{1}{\sqrt{2h}} \left( \sqrt{R^2 - b_{in}^2} + \sqrt{R^2 - b_{out}^2} + L_{int}(b_{in}, \varphi_{in}) \right)$$

$$(9) \quad = \frac{L_{int}(b_{in}, \varphi_{in})}{\sqrt{2h}} + \frac{2R}{\sqrt{2h}} + O\left(\frac{1}{R\sqrt{2h}}\right)$$

where  $\mathcal{L}(b_{in}, \varphi_{in})$  denotes the length of the orbit in  $S_R$  and  $L_{int}(b_{in}, \varphi_{in})$ , which is independent of  $R$ , roughly corresponds to the length of the trajectory in the interaction zone. The non-trivial dependence of  $t_{out}$  on the initial data is thus contained in  $L_{int}(b_{in}, \varphi_{in})$ . The scattering map may be written in terms of the impact coordinates so that only the travel time depends on  $R$ :

$$(10) \quad \mathcal{S}(R) : (b_{in}, \varphi_{in}) \rightarrow (b_{out}, \varphi_{out}, t_{out})$$

and (6) supplies the change of coordinates between the  $b$ 's and the  $s$ 's. Define the corresponding scattering functions at  $(b_{in}, \varphi_{in})$ :

$$(11) \quad (\Phi(b), T(b)) = (\varphi_{out}(b_{in} + b, \varphi_{in}), t_{out}(b_{in} + b, \varphi_{in})), \quad b \in J(b_{in}, \varphi_{in})$$

where  $J$  is either empty or a closed interval containing the origin such that for all  $b \in J(b_{in}, \varphi_{in})$  the scattering is non-trivial: the initial condition  $(b_{in} + b, \varphi_{in})$  does hit the scatterer. We say that  $(b_{in}, \varphi_{in})$  is *non-trivial* if  $J(b_{in}, \varphi_{in})$  is non-empty. Let

$$\mathcal{J}(b_{in}, \varphi_{in}) = \{(b, \varphi) | b = b_{in} + \bar{b}, \bar{b} \in J(b_{in}, \varphi_{in}), \varphi = \varphi_{in}\},$$

so that  $\Phi$  and  $T$  simply correspond to the first and third component of  $\mathcal{S}(R)|_{\mathcal{J}(b_{in}, \varphi_{in})}$ .

Let  $B$  denote the billiard map associated with the scatterers inside  $S_R$ . Let  $\chi$  parameterize the scatterers boundaries<sup>3</sup> and  $\theta \in [-\frac{\pi}{2}, \frac{\pi}{2}]$  the corresponding incidence angle, and let  $B(\chi, \theta) = (\chi', \theta')$  whenever the image of  $(\chi, \theta)$  under the billiard flow does not reach  $S_R$ . Denote by  $\Xi_{corner}$  the values of  $\chi$  at which corners appear (parameterizing  $\Gamma^*$ ). For any regular non-trivial  $(b_{in}, \varphi_{in})$ , we may write:

$$(12) \quad (b_{out}, \varphi_{out}) = S_{out} \circ B_k \circ B_{k-1} \circ \dots \circ B_1 \circ S_{in}(b_{in}, \varphi_{in}; R)$$

$$(13) \quad t_{out} = \frac{\mathcal{L}(b_{in}, \varphi_{in}; R)}{\sqrt{2h}},$$

where  $B_i = B(\chi_i, \theta_i)$  correspond to the interior billiard map whereas  $S_{in}$  and  $S_{out}$  correspond to the transition mapping from  $S_R$  to the first/last reflection values  $(\chi_1, \theta_1)$  and  $(\chi_k, \theta_k)$  respectively. More generally, for any non-trivial  $(b_{in}, \varphi_{in})$  an interior orbit may be defined:

$$(14) \quad O(b_{in}, \varphi_{in}) = \{\chi_i, \theta_i\}_{i=1}^k.$$

When  $k$  is finite and all the  $k$  reflections are regular (so  $\chi_i \notin \Xi_{corner}$  and  $\theta_i \neq \pm \frac{\pi}{2}$ ),  $(b_{in}, \varphi_{in})$  is a regular value. Then, the composition (12) results in a smooth  $C^r$  mapping with a smooth dependence of the scattering time  $t_{out}$  on initial conditions. Since for Sinai scatterers the set of initial conditions resulting in singular orbits is of measure zero, it follows that for Sinai scatterers, for almost all initial conditions, the map  $S$  is a smooth,  $C^r$  mapping. In principle, there are exactly two sources for non-smooth behavior of  $S$ : interior singularities that are associated with singular reflections from the scatterers and trapping singularities associated with the divergence of the number of interior reflections  $k$  (i.e.  $k \rightarrow \infty$ ).

**2.2. Interior billiard singularities.** For Sinai scatterers, the only interior singularities that may appear<sup>4</sup> are related to tangencies and to corners. Such singularities lead to non-smooth behavior and discontinuities in the scattering functions as explained next:

**2.2.1. Tangencies.** Assume the orbit  $O(b_{in}, \varphi_{in})$  is tangent to one of the scatterers at some point  $(\chi_t, \theta_t)$  (so  $\theta_t \in \{-\frac{\pi}{2}, \frac{\pi}{2}\}$ ), and contains no other singularities. Thus,  $k$  is finite, and for all  $i \neq t$  the reflections are regular. It follows that  $(b_{in}, \varphi_{in})$  belongs to a singularity line  $\Sigma_{tan}$  of initial conditions  $(b, \varphi)$  that have a tangency at the  $t$  iterate near  $(\chi_t, \theta_t)$ . A small neighborhood of  $\Sigma_{tan}$  is thus divided by  $\Sigma_{tan}$  to two parts - on one side of  $\Sigma_{tan}$  trajectories reflect exactly  $k$  times before escaping whereas on the other side trajectories have only  $k - 1$  reflections (see Fig. 1). Using the properties of the billiard map and flow near tangencies [40], it follows that the scattering map  $S$  is  $C^0$  (depends continuously yet not differentially on  $(b, \varphi)$ ) across such singularity lines (see Fig. 1). Such tangent singularity lines may intersect - the transverse intersection point of two<sup>5</sup> such lines corresponds to orbits with two tangencies. Notice that for regular orbits of the Sinai scatterers the universal Sinai cone property holds - the cones  $dq \cdot dp > 0$  are forward invariant, and their orientation is preserved under even number of reflections and reversed under odd number of reflections. This property implies that at regular values  $(b_{in}, \varphi_{in})$ , the function

<sup>3</sup>If there are  $N$  disjoint scatterers,  $\chi$  is a vector of  $N$  circles and a counter which points to the current component.

<sup>4</sup>For other scatterers, in addition to the possible appearance of non-hyperbolic invariant set, the transient behavior near focussing components (having whispering orbits), cusps, and deflection points needs to be analyzed.

<sup>5</sup>The (non-generic) intersection of  $p+2$  such lines corresponds to orbits with  $p+2$  tangencies and is expected to appear with  $p > 0$  only in non-generic cases: symmetric cases or higher co-dimension settings in which  $p$ -parameter families of scatterers are considered.

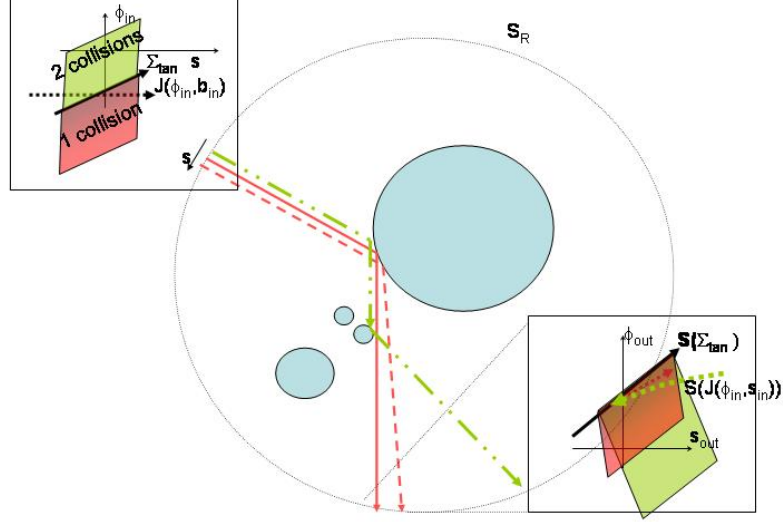


FIGURE 1. Scattering map and the effect of tangencies on it. The image of  $J(b_{in}, \varphi_{in})$  is not smooth and not monotone only at singular points, like this tangency.

$\Phi(b; b_{in}, \varphi_{in})$  is monotone whereas tangent values lead, in addition to the non-smoothness, to non-monotonicity (see Fig. 1).

**2.2.2. Corners.** Assume the orbit  $O(b_{in}, \varphi_{in})$  reaches a corner at its end point  $(\chi_k, \theta_k)$ , and contains no other singularities. Namely,  $k$  is finite,  $\chi_k \in \Xi_{corner}$ , and for all  $i < k$  the reflections are regular. Using the properties of the billiard map near regular corners (not cusps) [40], it follows that  $(b_{in}, \varphi_{in})$  belongs to a line  $\Sigma_c$  of singular values of  $(b, \varphi)$  all ending up at this corner point after  $k$  reflections. Initial conditions starting arbitrarily close to  $(b_{in}, \varphi_{in})$  on one side of this singularity line hit the upper boundary component near the corner, reflecting with some outgoing angle  $\theta_k^+$  and initial condition on the other side hit the lower boundary, reflecting with some outgoing angle  $\theta_k^-$ . Assume that the resulting two outgoing orbits are regular and escape to infinity. Then, in general, all the components of the scattering map  $S$  are discontinuous across  $\Sigma_c$ . Yet,  $S$  is well defined and smooth on either side of this singularity curve (in particular  $t_{out}$  has a finite value for all initial conditions that do not belong to  $\Sigma_c$ ). Other cases, for example, trapping of an outgoing orbit by redirecting into a corner (creating a corner polygon) or trapping by some components of the invariant set (creating a Corner- Hyperbolic Invariant Set - C-HIS - connection), are expected to appear at meeting points of  $\Sigma_c$  with additional components of the singularity set. Listing all such generic constructions deserves a separate study.

We denote by  $\Sigma_{bill} = \Sigma_{tan} \cup \Sigma_c$  the collection of singularity lines of initial conditions  $(b_{in}, \varphi_{in})$  that contain a billiard tangency or end up in a billiard corner.

**2.3. Trapping Singularities.** The singularities associated with the divergence of  $k$  (i.e. when  $k \rightarrow \infty$ ) are caused by orbits that asymptote the billiard's invariant set, its corner polygons or its C-HIS and HIS-C connections (it appears that only the first possibility was previously considered); Denote by  $\Lambda$  the generalized invariant set of  $B$ , which includes, in addition to the proper invariant set, all these singular semi-orbits. Denote by  $\Sigma_\Lambda$  the set of initial conditions  $(b_{in}, \varphi_{in})$  that never escape, so  $k = \infty$  for these orbits and  $S$  is not defined for them. The set  $\Sigma_\Lambda$  contains all the initial conditions belonging to stable manifolds of the hyperbolic component of the invariant set,  $\Lambda_h$ , and, if  $\Lambda$  has non-hyperbolic components or includes singular semi-orbits, it may contain other non-hyperbolic sticky orbits or orbits that asymptote singularities.

**2.4. Scattering functions and singularities for Sinai scatterers.** Summarizing, let  $\Sigma$  define the set of all singular initial condition on  $(b_{in}, \varphi_{in}) \in (-R, R) \times [0, 2\pi)$ :

$$\Sigma = \Sigma_{bill} \cup \Sigma_\Lambda.$$

Then, for Sinai scatterers,  $S$ ,  $\Phi$  and  $T$  are smooth and monotone away from the singularity lines composing  $\Sigma$ . Generically, these singularity lines cross the segment  $\mathcal{J}(b_{in}, \varphi_{in})$  transversely. In the simplest case  $\Sigma_{bill}$  crosses  $\mathcal{J}(b_{in}, \varphi_{in})$  at isolated points<sup>6</sup>, that correspond to simple tangent escaping orbits or to simple corner semi-orbits. The scattering functions  $S$ ,  $\Phi$  and  $T$  are finite, continuous yet not smooth and non-monotone (respectively, are discontinuous, and, depending on the corner properties and on  $\varphi_{in}$ , may be monotone or non-monotone, see [44] and Fig. 3), across such isolated intersections of  $\mathcal{J}(b_{in}, \varphi_{in})$  with the singularity line  $\Sigma_{tan}$  (respectively, with  $\Sigma_c$ ). Finally, near  $\Sigma_\Lambda$  we will always have an accumulation of singularities. Near the intersection of  $\mathcal{J}(b_{in}, \varphi_{in})$  with the singularity lines corresponding to initial conditions belonging to the stable manifold of the hyperbolic component of  $\Lambda$ ,  $\Sigma_{\Lambda_h}$ , the scattering functions have self similar structure and a diverging  $T$ . The behavior near other components of  $\Sigma_\Lambda$  is yet to be studied.

**2.5. Regular and Singular Sinai Scatterers.** The Sinai scatterer  $D$  will be called *regular* if it has no corners and its invariant set  $\Lambda$  is bounded away from the singularity set so it is uniformly hyperbolic<sup>7</sup>. In such a case,  $\Lambda$  is structurally stable - a sufficiently small smooth deformation of  $D$  does not change the symbolic dynamic description of the dynamics on  $\Lambda$  nor its hyperbolic structure. The Sinai scatterer is *singular* when  $\Lambda$  contains any singular orbits (tangent orbits) or singular semi orbits (corner polygons or C-HIS and HIS-C connections).

Most of the studies of chaotic scattering by billiards were performed for regular Sinai scatterers [30]. Then, the hyperbolic structure of  $\Lambda$  implies that for most  $(b_{in}, \varphi_{in}) \in \Sigma_\Lambda$ , the image under sufficiently many reflections of a small neighborhood of  $\mathcal{J}(b_{in}, \varphi_{in})$  aligns along the unstable manifold of  $\Lambda$  and thus inherits all its self-similar, fractal and hyperbolic properties [14][42],[13],[29].

When the invariant set  $\Lambda$  undergoes a bifurcation, the Sinai scatterer is singular, and the above description is no longer valid; For example, in the classical three disc scatterer

<sup>6</sup>In a family of segments, there may also appear some isolated  $(b_{in}, \varphi_{in})$  values at which two of the singularity lines and  $\mathcal{J}(b_{in}, \varphi_{in})$  cross, namely a triple intersection appears.

<sup>7</sup>The classical example of three identical circular scatterers of radius  $a$  centered on the vertices of an equilateral triangle with edges of length  $R$  is a regular Sinai scatterer for  $R > 3a$ : then the invariant set  $\Lambda_h$  is bounded away from any tangent trajectory, and  $\Lambda_h$  is fully described by symbolic dynamics on 3 symbols with a simple transition matrix [14].

problem, when the equi-distance between the discs,  $R$ , is decreased towards their radius  $a$ , orbits in  $\Lambda$  undergo tangent bifurcations<sup>8</sup>, a more detailed partition is needed, and the transition matrix becomes more complex, till, in the limit of  $R = a$  (which is not a Sinai scatterer since cusps are created), infinite partition is achieved and the invariant set has a full measure [14].

In section 3 we show that the smooth flow scattering properties can be predicted by studying the simpler billiard scattering problem. To this aim, we first prove that steep smooth flows limiting to regular Sinai scatterers have similar scattering properties to the billiards'. On the other hand, we show that near singular Sinai scatterers the smooth scattering is inherently different, yet predictable. To demonstrate the latter effect we choose two geometrical settings, inspired by [44, 33, 35]: the first corresponds to a billiard geometry with a tangency and the second to one with corners (see Figure 2). The choice of symmetric configurations helps to pinpoint the source for the altered behavior - the singularity leads to the emergence of symmetric stable periodic orbits in the invariant set of the smooth flow.

*2.5.1. The symmetric four discs scatterer – scatterers with tangent invariant orbits.* Consider one large circle  $\Gamma_0$  of radius  $R$  which is centered at  $(x_0^c, y_0^c) = \left(\frac{L}{\sqrt{2}}, \frac{L}{\sqrt{2}}\right)$ , one intermediate circle  $\Gamma_1$  of radius  $r$  which is centered at  $(x_1^c, y_1^c) = (0, 0)$ , and 2 small circles  $\Gamma_{2,3}$  of radius  $r/2$  arranged with centers along the line  $y = -x + 1$  at a fixed distance  $2Kr$  apart. Denote by  $\mu r$  the distance of  $\Gamma_2$  from the diagonal, so that at  $\mu = 0$  the diagonal is tangent to  $\Gamma_2$ , and at  $\mu = K$  the circles  $\Gamma_{2,3}$  are placed symmetrically with respect to the line  $y = x$  (see Figure 2C,D). The four<sup>9</sup> disc geometry corresponds to a regular Sinai billiard when the discs are placed sufficiently far from each other ( $K$  and  $L$  are sufficiently larger than  $r$ ), and sufficiently away from co-linear configurations (a line passing through any two discs is at a large distance from any other disc, namely,  $\frac{K}{L} = O(1)$ ). Here, we examine the behavior near a singular Sinai scatterer configuration, where  $\frac{K}{L} \ll 1$ , so the invariant set has close to tangent trajectories (hereafter we fix  $R = 10r, L = 13r, K = 0.1r, r = 1$ ). At  $\mu = 0$  the invariant set has a tangent periodic orbit (Fig. 2D), whereas we expect that for most values of  $\mu > 0$  the invariant set is non singular, thus hyperbolic, producing self-similar structure with positive fractal dimension which is less than one as in [14],[42],[13],[29] (see also the bottom plot of Fig. 12).

*2.5.2. The pearly scatterer – Scatterers with corners:* Consider a large circle  $\Gamma_0$  of radius  $R$  which is centered at  $(x_0^c, y_0^c) = \left(\frac{L}{\sqrt{2}}, \frac{L}{\sqrt{2}}\right)$  and  $n$  small circles  $\Gamma_1, \dots, \Gamma_n$  of radius  $r_n$ , covering uniformly an interval of length  $r = 1$ , see<sup>10</sup> Fig. 2A,B. The radius  $r_n(\alpha)$  is chosen so that the angle  $\alpha$  between any two neighboring circles<sup>11</sup> is independent of  $n$ :

$$(15) \quad \alpha = \pi - \arccos(1 - 2(1 - \mu^2)), \quad r_n = \frac{1}{2(1 + (n-1)\sqrt{1 - \mu^2})}, \quad \mu \in [0, 1].$$

<sup>8</sup>Probably, for some parameter intervals, on a dense set of parameter values; See [43] for a numerical evidence to the appearance of tangent homoclinic orbits on a dense set of parameters in a Sinai billiard.

<sup>9</sup>For convenience we choose the four discs example and not the classical three discs example. Here, we can examine the simple symmetric configuration at  $\mu = K$ .

<sup>10</sup>The case  $n = 2$  was generalized in a different manner to multi-dimensional geometries in [33][35].

<sup>11</sup>The angle between the tangent lines at the point of the intersection of the circles

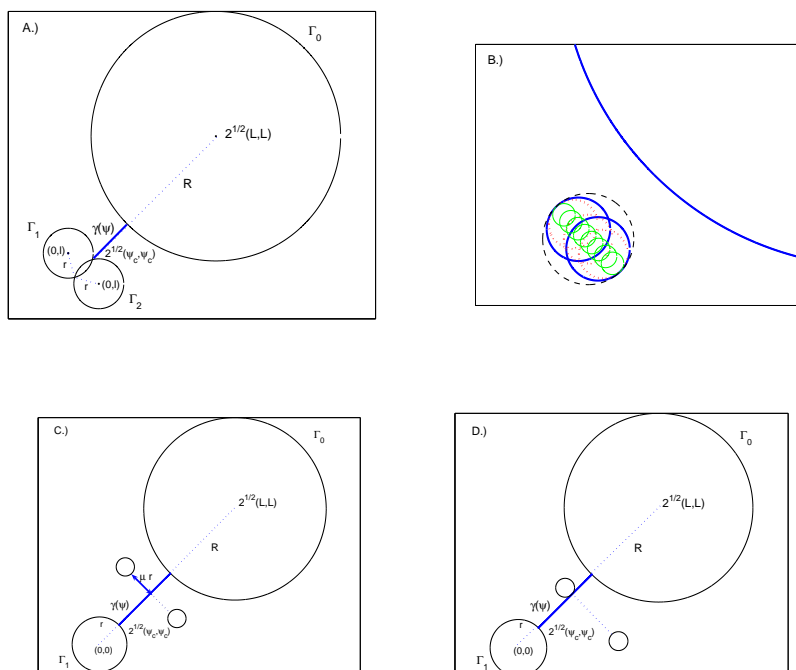


FIGURE 2. The geometries of the two singular Sinai scatterers. A) The pearly billiard with one corner. B) The pearly billiard with  $n - 1$  corners: dashed (black)  $n = 1$ , bold (blue)  $n = 2$ , dotted bold (red)  $n = 3$ , solid (green)  $n = 8$ . C) The symmetric four discs case ( $\mu = K$ ). D) The non-symmetric tangent case:  $\mu = 0$ .

The centers of the small circles lie on the line  $y = -x + \frac{1}{\sqrt{2}} \left( \frac{\sqrt{1-\mu^2}}{\sqrt{1-\mu^2+1}} \right)$ . Hereafter we fix  $R = 10r, L = r * (12 + \mu + \sqrt{1 - \mu^2}), r = 1$  and vary  $n$  and  $\mu$ .

This is a singular Sinai scatterer for any finite  $n$  and  $\mu > 0$ . The geometrical deformation of the scatterers depend smoothly on  $\mu$  for all  $\mu \neq 1$ . Following the same procedure as in [14], for most values of  $\mu \in (0, 1)$  one may fully characterize the invariant set using symbolic dynamics in which the  $n + 1$  symbols  $\{0, 1, \dots, n\}$  encode the order of the collisions with the circles  $\Gamma_i$ , and, since the circles are dispersing, the sequence  $\Gamma_i \Gamma_i$  is always forbidden. The detailed phase space partition and the corresponding transition matrix depend on  $\mu$  in a non-trivial fashion; For  $\mu$  values that are close to 1 we expect that the symbolic sequences in the invariant set will be simple and consist of pairs of collisions of the form  $\Gamma_i \Gamma_0$  with  $i \neq 0$  (for such  $\mu$  values collisions between neighboring small circles,  $\Gamma_i \Gamma_{i \pm 1}$  with  $i, i \pm 1 \neq 0$ , will be subsequently reflected to infinity and will not belong to the invariant set). On the other hand, for small  $\mu$ 's, sequences of the form  $\Gamma_i \Gamma_{i+1} \Gamma_i \dots \Gamma_{i+1} \Gamma_0$  with preamble of varying length of up to  $\left\lfloor \frac{\pi}{\alpha(\mu)} \right\rfloor$  collisions between the neighboring scatterers  $\Gamma_i$  and  $\Gamma_{i+1}$  are expected to emerge (so that in the limits of  $\mu \rightarrow 0$  an infinite partition is needed).

The study of the topological changes of the invariant set as  $\alpha(\mu)$  crosses the rational angles  $\pi/m$  is interesting and may be conducted using the standard geometrical methods.

Fig. 3 demonstrates some of these corner effects for  $\mu = 0.9$  and several  $n$  values. It clearly shows that each additional corner leads to an additional unresolved region, a property that is kept under the self-similar magnification. It also demonstrates that the scattering functions are indeed *discontinuous* across  $\Sigma_c$ . Fixing  $n = 3$  and  $\mu = 0.9$  we supply further details regarding the scattering of an incoming ray of initial conditions; as common we divide this ray to resolved (trajectories escaping after one or two reflections) and unresolved (trajectories remaining close to the stable manifold of the unstable periodic orbits) intervals (see Figure 3 and the right part of Figure 3.  $\bar{R}$  is taken sufficiently large to enclose the scatterer, hereafter  $\bar{R} = 10(R + L)$ ):

Interval	T	Collisions	Resolved/Unresolved	Color
$I_1$	2	$\Gamma_0\Gamma_nS_{\bar{R}}$	R	green
$I_2^j$	$\geq 2$	$\Gamma_0\Gamma_j\dots(j = 1, \dots, n)$	U	blue
$I_3$	2	$\Gamma_0\Gamma_1S_{\bar{R}}$	R	green
$I_4$	1	$\Gamma_0S_{\bar{R}}$	R	red
$I_5^j$	$\geq 2$	$\Gamma_n\Gamma_0\Gamma_j\dots(j = 1, \dots, n)$	U	blue
$I_6$	2	$\Gamma_n\Gamma_0S_{\bar{R}}$	R	green
$I_7$	1	$\Gamma_nS_{\bar{R}}$	R	red

On the resolved intervals  $I_{1,3,4,6,7}$  the scattering function is smooth and monotone, as expected. The left part of Fig. 4 shows the geometry of the corresponding trajectories. The unresolved intervals  $I_{2,5}^j$  may be further subdivided to  $n$  unresolved regions according to their next collision with a small circle  $\Gamma_i$ , and this process can be further repeated in a self-similar manner, namely, for this  $\mu$  value a fully chaotic scattering is developed for  $n \geq 2$ .

Since all the trapped trajectories at  $\mu = 0.9$  consist of pairs  $\Gamma_0\Gamma_j$  (with  $j \neq 0$ ), the magnification factor depends linearly on the curvature of the small circles (15) (see the right part of Figure 4, where, for  $n \leq 10$  and a fixed  $\mu = 0.9$  we obtain:  $\log(M(n); \mu = 0.9) \approx 1.3 + \log(1/r_n)$ ). Moreover, the growth factor in the number of unresolved intervals at this value of  $\mu$  is observed to be  $n$ . Thus, the fractal (box-counting) dimension of the singularity set is estimated by

$$(16) \quad F(n; \mu = 0.9) = \frac{\log(n)}{\log(M(n), 0.9)} \approx \frac{\log(n)}{1.3 + \log(1/r_n)},$$

where  $r_n$  is defined by (15). The dependence of this expression on  $\mu$  and larger  $n$  values is yet to be explored; From (15) we conjecture that this fractal dimension approaches 1 as  $n$  is increased at a fixed  $\mu$  value (a somewhat expected result - the boundary of the scatterer becomes non-smooth in this limit). When  $\mu$  crosses a bifurcation value (e.g. when  $\alpha(\mu) = \pi/m$ ) the partition is altered and one may expect the growth factor to change as well.

### 3. SCATTERING BY STEEP POTENTIALS

**3.1. Formulation.** Consider the smooth two-dimensional Hamiltonian flow (1) with the steep, billiard-like potential  $W(q; \varepsilon)$  [38], that limits, as  $\varepsilon \rightarrow 0$ , to the hard wall scatterer problem in  $\mathcal{D} = S_R^{interior} \setminus D$ . For a fixed  $R$ , in analogy to (5), the return map by the smooth

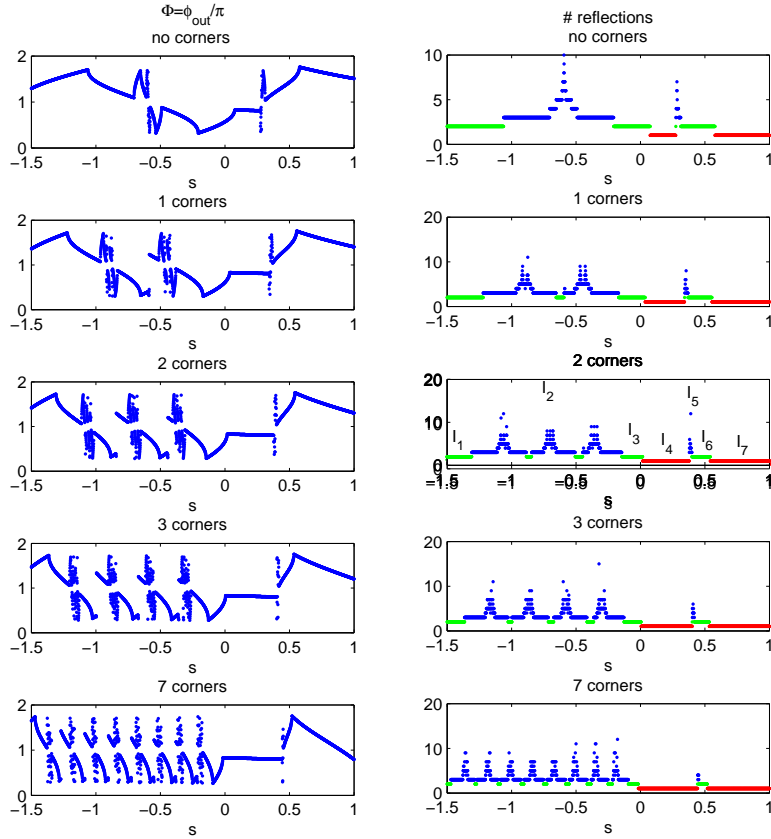


FIGURE 3. Scattering function for the  $n$ -pearls scatterer,  $\Phi_n(s)$  and the corresponding number of reflections  $T_n(s)$  ( $T = 1$  red,  $T = 2$  green,  $T \geq 2$  blue) for different values of  $n$ .

flow to the section  $q \in S_R$  defines the corresponding scattering map of the smooth flow<sup>12</sup>:

$$S^\varepsilon(R) : (s_{in}, \varphi_{in}) \rightarrow (s_{out}^\varepsilon, \varphi_{out}^\varepsilon, t_{out}^\varepsilon).$$

For a fixed  $R$ , conditions I-IV of [38, 34] on  $W(q; \varepsilon)$  in  $\mathcal{D}$ , that are included in the appendix for completeness, suffice to insure that regular reflections of  $S(R)$  are inherited by  $S^\varepsilon(R)$ ; Roughly, we require  $W(q; \varepsilon)$  to asymptotically vanish away from the scatterer, we require that the level sets of  $W(q; \varepsilon)$  approach smoothly the scatterer boundary and that the normal force on these level sets is repelling so that the time spent in the boundary layer around each of these scatterer is small and depends smoothly on the initial conditions. In particular, if

<sup>12</sup>The relation to the Poincaré scattering map, defined in analogy to the quantum  $S$ -matrix (see [20]), may be found, provided the potential decays sufficiently rapidly away from the scatterers, by using the impact coordinates.

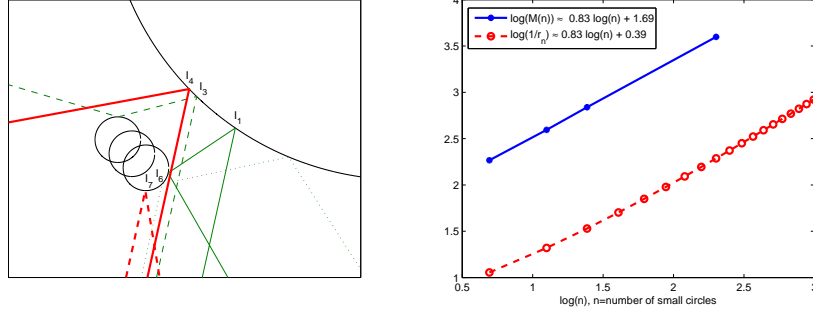


FIGURE 4. Left: The trajectories corresponding to the intervals of initial conditions  $I_1$  (solid),  $I_3$  (dashed),  $I_4$  (bold),  $I_6$  (dotted),  $I_7$  (bold dashed). Right: The magnification factor and the curvature of small circles as a function of  $n$  in log scale.

the potential is of the form:

$$(17) \quad W(q; \varepsilon) = \sum_{i=1}^N \mathcal{E}_i V\left(-\frac{Q_i(q)}{\varepsilon}\right).$$

where  $Q_i(q)|_{q \in \partial D_i} = 0$ ,  $Q_i(q)|_{q \in \mathcal{D}} > 0$ ,  $\mathcal{E}_i \geq \mathcal{E} > 0$ ,  $N$  is finite, and there exists an  $\alpha > 0$  such that the smooth function  $V$  satisfies<sup>13</sup>:

$$(18) \quad V(0) \geq 1, V(z) > 0, V(z) = O_{C^{r+1}}\left(\frac{1}{z^\alpha}\right) \text{ for } z \gg 1,$$

then these conditions are satisfied. For example, the  $V$  may be taken to be the exponential function  $V = \exp(-\frac{Q}{\varepsilon})$ , the Gaussian function  $V = \exp(-\frac{Q^2}{\varepsilon^2})$  or a power-law  $V = \left(\frac{\varepsilon}{Q}\right)^\alpha$  potential with some  $\alpha > 0$ .

We also note that conditions I-IV listed in the appendix imply that for all  $h \in (0, \mathcal{E})$  and sufficiently small  $\varepsilon$  (non-uniformly in  $h$ ), the Hill's region in  $S_R$ , has the same topology as  $\mathcal{D}$ . Equivalently, let  $W_{\max}(\varepsilon), W_{\min}(\varepsilon), W_{\text{sad}}(\varepsilon)$  and  $W_{\max-R}(\varepsilon)$  be the sets of the potential values at its local maxima, minima and saddle points in  $\mathcal{D}$ , and its maximal value on  $S_R$ , respectively. Notice that

$$\{W_{\max}(\varepsilon), W_{\min}(\varepsilon), W_{\text{sad}}(\varepsilon), W_{\max-R}(\varepsilon)\} \rightarrow \{V(0)\mathcal{E}_i, 0, 0, 0\} \text{ as } \varepsilon \rightarrow 0.$$

so, there exists  $\varepsilon_{\max}(h)$  such that for any  $\varepsilon \in (0, \varepsilon_{\max}(h))$ , the local maxima values,  $\{W_{\max}(\varepsilon)\}$ , are all larger than  $h$  and all the other extremal points are below  $h$ :

$$\max\{W_{\min}(\varepsilon), W_{\text{sad}}(\varepsilon), W_{\max-R}(\varepsilon)\} < h < \min\{W_{\max}(\varepsilon)\}, \text{ for all } \varepsilon \in (0, \varepsilon_{\max}(h)).$$

Thus,  $\varepsilon_{\max}(h)$  serves as an upper bound for  $\varepsilon$  values for which the current approach may be applicable<sup>14</sup> - for  $\varepsilon > \varepsilon_{\max}(h)$  the topology of the Hill's region of the smooth flow is different than the topology of  $\mathcal{D}$ , see Fig. 5.

<sup>13</sup>By  $O_{C^{r+1}}\left(\frac{1}{z^\alpha}\right)$  we mean that the  $r$  derivatives of  $V$  decay at least as fast as the corresponding  $r+1$  derivatives of  $\frac{1}{z^\alpha}$ .

<sup>14</sup>The auxiliary billiard, defined in [34] (see also the appendix), may be a useful concept for such  $\varepsilon$  values.

**3.2. Closeness theorems.** For steep potentials satisfying conditions I-IV, the results of [43, 38, 44, 34, 33, 35] regarding the relations between the billiard orbits in  $\mathcal{D}$  and the smooth flow in this domain are valid. In the appendix, we include several theoretical results that follow directly from these works. In particular, we establish there that for such potentials, if  $(s_{in}(b_{in}, \varphi_{in}; R), \varphi_{in})$  is a non-trivial regular value (respectively,  $(s_{in}, \varphi_{in}) \in \Sigma_{\text{tan}}$  has a finite number of collisions, one tangent and all the rest regular) of the billiard scattering map  $S$ , then there exists a nearby initial condition  $(s_{in}^\varepsilon, \varphi_{in}^\varepsilon)$ , limiting to  $(s_{in}, \varphi_{in})$  as  $\varepsilon \rightarrow 0$ , such that the smooth scattering map  $S^\varepsilon$  is  $C^r$  close<sup>15</sup> (respectively, is  $C^0$  close) to  $S$  at  $(s_{in}, \varphi_{in})$ . Furthermore, error estimates for the closeness of such smooth and billiard trajectories are established. The most important corollary that follows from such results is that for regular Sinai scatterers the smooth flow and the billiard scatterer have the same scattering properties:

**Corollary 1.** *Consider a Hamiltonian system with a potential  $W(q, \varepsilon)$  satisfying Condition **I-IV** in the domain  $\mathcal{D} = S_R^{\text{interior}} \setminus D$ , where  $D$  is a **regular Sinai scatterer** so that  $\Lambda$  is a non-trivial uniformly hyperbolic invariant set of  $B$ . Then, for sufficiently small  $\varepsilon$ , (1) has a uniformly hyperbolic invariant set  $\Lambda^\varepsilon$  belonging to the energy level  $h \in (0, \mathcal{E})$  which is topologically conjugate to  $\Lambda$ . Moreover, the local stable and unstable manifolds of  $\Lambda^\varepsilon$  are  $C^r$  close to the local stable and unstable manifolds of  $\Lambda$ .*

Thus, we expect that under these conditions, the self-similar structure and the fractal dimension of the scattering functions of the smooth flow will limit to the corresponding structures of the billiard scatterers. These positive conclusions, that allow to approximate smooth flows by billiards, are natural and are clearly observed in various simulations (e.g. see appendix and Fig. 11). We do note though that without the machinery developed in [43, 34] it is not obvious how to prove such results in the general case: the limit of the smooth flow to the billiard flow is singular (e.g. the vector fields associated with these two flows are not close even in the  $C^1$  topology).

For example, to study the problem of motion in the  $n$  centers Coloumbic potentials, a sophisticated and beautiful mathematical set up was developed to prove that in the high energy limit the invariant set is hyperbolic provided the centers are not co-linear [22]. We propose that by introducing another fictitious radius parameter as in [7], the above corollary may be used to construct an additional proof of this result for the repelling case. Moreover, the current tools may be employed to detect configurations and (high) energy levels at which the invariant set in the repelling Coulombic case is non-hyperbolic.

#### 4. BILLIARD SINGULARITIES AND STEEP POTENTIAL SCATTERING

The above persistence results are expected to fail for singular Sinai scatterers. Indeed, in [43, 38, 44] it was established that tangent and corner singularities of the billiard lead to stable orbits of the smooth flow. Thus, we expect that when  $\Lambda$  has such singularities the smooth flow and the billiard will have a substantial different scattering functions.

To demonstrate these effects we consider two families of Hamiltonian flows that limit to the two geometrical settings introduced in sections 2.5.1 and 2.5.2. More precisely, we consider two-parameter families of Hamiltonian flows (1):

$$(19) \quad H = \frac{p_x^2}{2} + \frac{p_y^2}{2} + W(x, y; \mu, \varepsilon),$$

<sup>15</sup>Namely, for small  $(s, \varphi)$ , for sufficiently small  $\varepsilon$ ,  $S^\varepsilon(s_{in}^\varepsilon + s, \varphi_{in}^\varepsilon + \varphi) - S(s_{in} + s, \varphi_{in} + \varphi)$  and the  $r$  derivatives of this map with respect to  $(s, \varphi)$  are small.

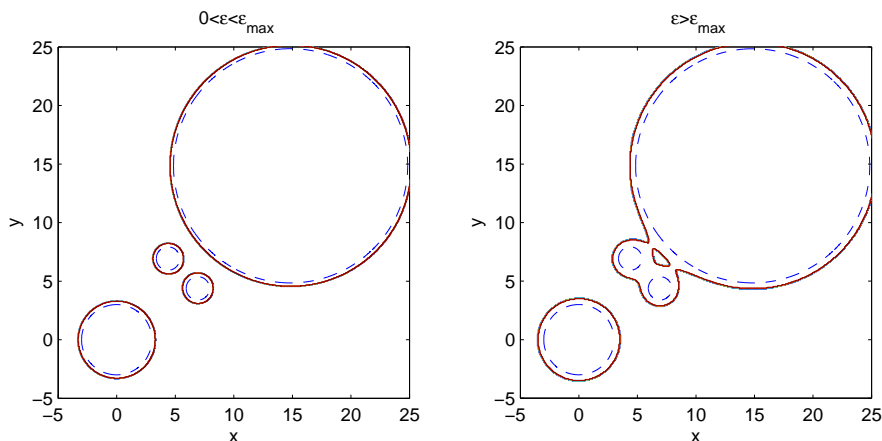


FIGURE 5. The level set of the exponential potential at  $h = \frac{1}{2}$  for  $\varepsilon = 0.3 \in (0, \varepsilon_{\max}(\frac{1}{2}) = 0.6)$  (left) and  $\varepsilon = 0.75 > \varepsilon_{\max}$  (right). The dotted circles correspond to the billiard limit.

where  $\varepsilon$  controls the steepness of the potential and  $\mu$  controls the billiard geometry: in the four-disc case  $\mu$  controls the distance of the diagonal orbit from tangency (see section 2.5.1), whereas for the pearly scatterers  $\mu$  controls the angle between the neighboring small discs. We choose the potential  $W$  to be of the form (3):

$$(20) \quad W_{\text{corner}}(q; \varepsilon) = \exp\left(-\frac{Q_0(q)}{\varepsilon}\right) + \frac{1}{n} \sum_{k=1}^n \exp\left(-\frac{Q_k(q)}{\varepsilon}\right);$$

$$(21) \quad W_{\text{tangent}}(q; \varepsilon) = \sum_{k=0}^3 \exp\left(-\frac{Q_k(q)}{\varepsilon}\right),$$

where  $Q_j(q)$  (the pattern function of [34]) is the distance between  $q = (x, y) \in \mathcal{D}_{\text{Hill}}(h, \mu, \varepsilon)$  and the circle  $\Gamma_j$ , where  $\mathcal{D}_{\text{Hill}}(h, \mu, \varepsilon)$  denotes the Hill's region. The exponential potential is chosen for convenience and may be replaced by any other steep billiard-like potential satisfying assumption I-V. The  $\varepsilon$  values we consider are sufficiently small to insure that at the energy level  $h = 1/2$  there are no abrupt bifurcations, namely the topology of  $\mathcal{D}_{\text{Hill}}(h, \mu, \varepsilon)$ , is unchanged for these  $\varepsilon$  values, see Fig. 5.

According to [43, 38, 44], in each of these two geometries we expect to have wedges in the  $(\mu, \varepsilon)$  plane, emanating from isolated  $(\mu^*, 0)$  values, such that the smooth flow has stable periodic orbit for all parameters in these wedges, see Fig. 6. In principle, the location of the periodic orbit and the extent of the stability zone may be explicitly found using the perturbation methods developed in these works. Utilizing the symmetric geometrical construction simplifies the analysis and the computations as explained next.

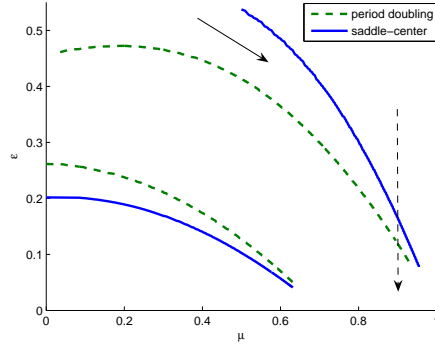


FIGURE 6. Wedges of stability for the smooth one-corner case ( $n = 2$ ). Dashed arrow shows the parameter values taken in figure 8. Solid arrow indicates a possible choice of a curve  $(\mu(\epsilon), \epsilon)$  along which stability islands exist for arbitrary small  $\epsilon$  values.

4.1. **Stable symmetric periodic orbit.** Let  $\{\gamma(\psi) = \frac{1}{\sqrt{2}}(\psi, \psi) \mid \psi \in (\psi_c, L - R)\}$  denote the diagonal line for both geometries (see Fig. 2). The diagonal  $\gamma$  intersects  $\Gamma_0$  in the normal direction and has another point of intersection  $\gamma(\psi_c) = \frac{1}{\sqrt{2}}(\psi_c, \psi_c)$ . In the tangent case  $\gamma(\psi_c)$  is the point of the normal intersection of  $\gamma$  with  $\Gamma_1$  (Fig. 2C), so, for all  $\mu > 0$ ,  $\gamma$  corresponds to a regular hyperbolic orbit, whereas at  $\mu = 0$  it is tangent to the boundary. In the one corner case ( $n = 2$ ),  $\gamma(\psi_c)$  is the intersection point of the two small circles (Fig. 2A), thus, for all  $\mu$  and  $L > R + \psi_c$ ,  $\gamma$  corresponds to a simple corner polygon of the billiard.

For the smooth Hamiltonian, in the symmetric case (i.e. for any  $\mu$  in the corner case and for  $\mu = K$  in the tangent case), the motion along the diagonal is invariant. It follows that for sufficiently small  $\epsilon$ , a periodic orbit  $\gamma(\psi, \epsilon)$  is created. Its stability properties are examined, using the numerical techniques<sup>16</sup> developed in [33] and [35], by computing the Monodromy matrix of the local Poincaré map near this orbit. For the corner geometry, this construction could be repeated for any even number of small circles, but here we study only the  $n = 2$  case.

As predicted by [38][44], we indeed find that in both cases, for a fixed value of  $\mu$  there exists an interval of  $\epsilon$  values where the periodic orbit  $\gamma(\psi, \mu, \epsilon)$  is elliptic: the real part of the two eigenvalues of the Poincaré map lie in the interval  $[-1, 1]$ , where 1 corresponds to the saddle-center bifurcation and  $(-1)$  to the period doubling bifurcation.

For the tangency case we take  $K = 0.1$  (i.e. the distance between the two small circles is  $0.2r$ ) and  $\mu = K = 0.1$  so that the Hamiltonian is symmetric with respect to a reflection about the diagonal. Fig. 7A shows that there are several intervals of stability appearing at this  $\mu$  value. In particular, the reference points at  $\epsilon = 0.5, 0.258, 0.03$  present values that are far from the stability wedges (so  $|\text{Re}(\lambda)| \gg 1$ ), the values  $\epsilon = 0.44, 0.152$  reside inside the stability intervals, and the values  $\epsilon = 0.449, 0.425$  are close to the stability interval boundaries. The phase portraits of the Poincaré map near  $\gamma(\psi, 0.1, \epsilon)$  are shown in Fig. 7B - in these figures the stability islands are clearly observed.

For the corner case we take  $\mu = 0.9$  (i.e.  $\alpha \approx 0.7\pi$ ), where the invariant set does not appear to have neighboring reflections (see section 2.5.2). Taking reference points above

<sup>16</sup>see also [35] for analytical results in a similar setting.

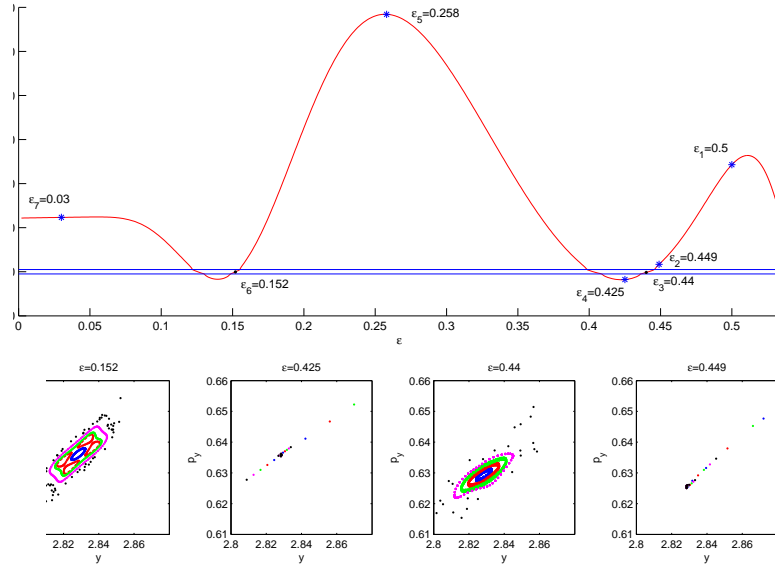


FIGURE 7. A) The real part of  $\lambda$  for the tangent case  $\mu = K = 0.1$ . B) The phase spaces  $y$  vs.  $p_y$  for  $\epsilon$  values shown on A).

the interval of stability  $\epsilon = 0.4698, 0.1842$ , inside the interval  $\epsilon = 0.1403$ , close to the period doubling boundary  $\epsilon = 0.1146$  and below the interval  $\epsilon = 0.06654, 0.01$  we again obtain numerically that in and near the stability wedges elliptic islands appear, whereas away from the wedges, hyperbolic escape from the vicinity of  $\gamma(\psi, \mu, \epsilon)$  is observed (see Figure 8B).

**4.2. Scattering by steep potentials near the billiard singularities.** To demonstrate the effects of the changes in the invariant set on the scattering functions, we compute these for  $\epsilon$  values below, inside, and above the stability wedges for both the corner and tangent geometries. The results of these computations are shown in figures 9-11. Figure 9 shows the scattering function for the corner geometry with  $n = 2$  and  $\mu = 0.9$  for the  $\epsilon$  values shown in Fig. 8. Detailed examination of the structure of these scattering functions suggests the following scenario:

- (1) The billiard scattering at  $\mu = 0.9$  is chaotic and its invariant set appears to be uniformly hyperbolic: as shown on the right part of Fig. 11, the regions that exhibit self-similar behavior are bounded away from the discontinuity point that is associated with the corner. Thus, the billiard scattering function exhibits the typical self-similar structure discussed in section 2.5.2.
- (2) At  $\epsilon = 0.01$  the scattering function resembles the chaotic billiard scattering function and possesses the same type of self-similarity (Fig. 11 left). We propose that this observation is closely related to corollary 1: since the scattering near the invariant set is regular hyperbolic and  $\epsilon$  is sufficiently small the invariant set persists, and the self-similar structure of its local stable manifold persists as well. On the other hand, in corollary 1 corners were not allowed. Indeed, since the diagonal represents a possible mechanism for a recurrent motion near the corner (a valid corner polygon, see [44]), the invariant set of the smooth flow has this *additional*

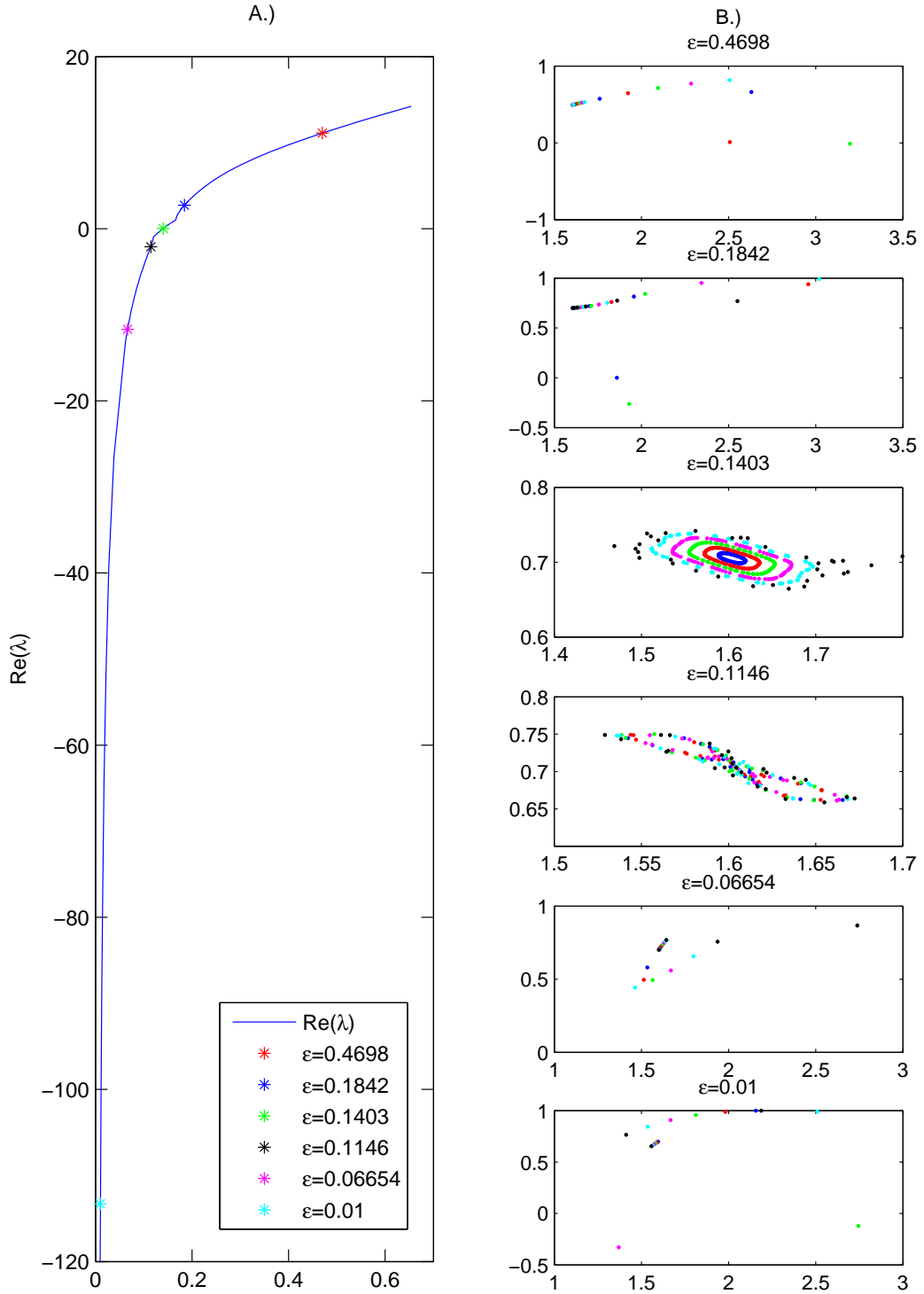


FIGURE 8. A) The real part of  $\lambda$  for the corner case  $n = 2, \mu = 0.9$ . B) The phase spaces  $x$  vs.  $p_x$  for  $\epsilon$  values shown on A).

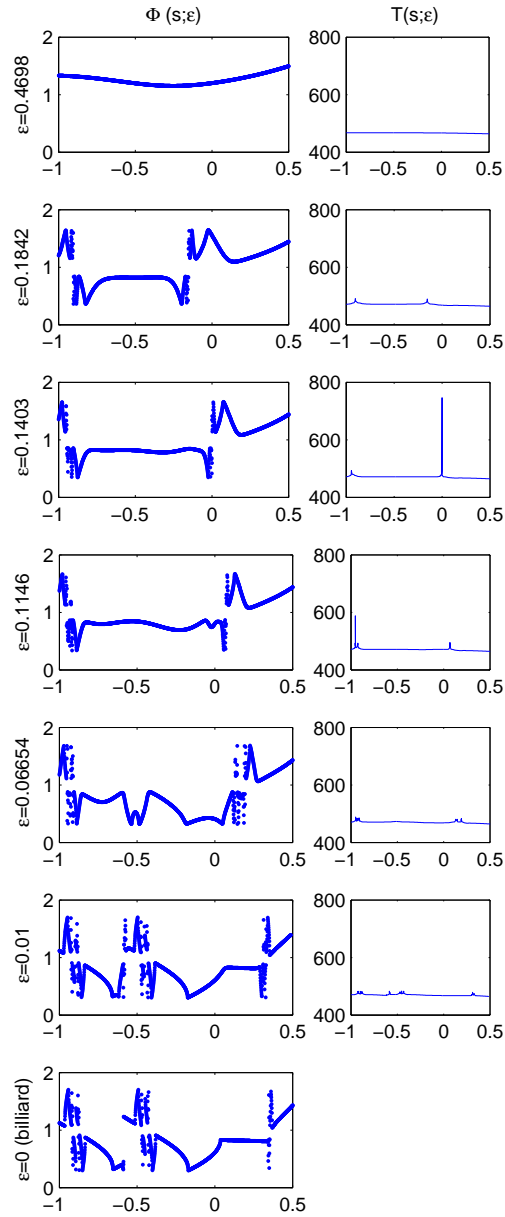


FIGURE 9. Scattering function  $\Phi_2(s; \epsilon)$  and  $T_2(s; \epsilon)$  for the pearly case with  $n = 2$ .

*new component* - the diagonal orbit, which, for this value of  $\epsilon$ , is hyperbolic. We see that the scattering function of the smooth flow has an additional unresolved region of non-monotonicity associated with this diagonal orbit, and thus, we expect that the smooth flow will develop some non-hyperbolic behavior near this

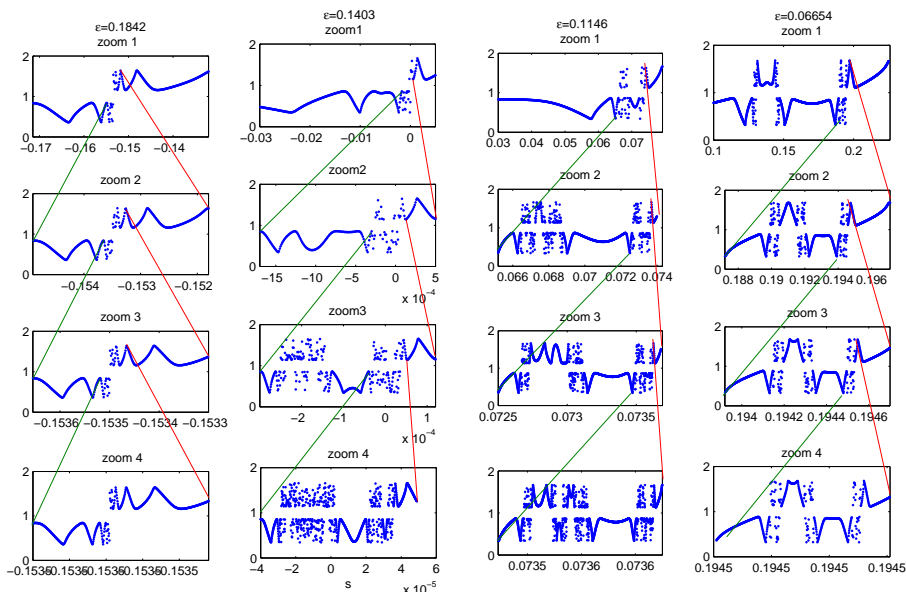


FIGURE 10. Close-up of the unresolved region of  $\Phi_2(s; \epsilon)$  near the right unresolved region for  $\epsilon = 0.1842, 0.1403, 0.1146, 0.06654$ .

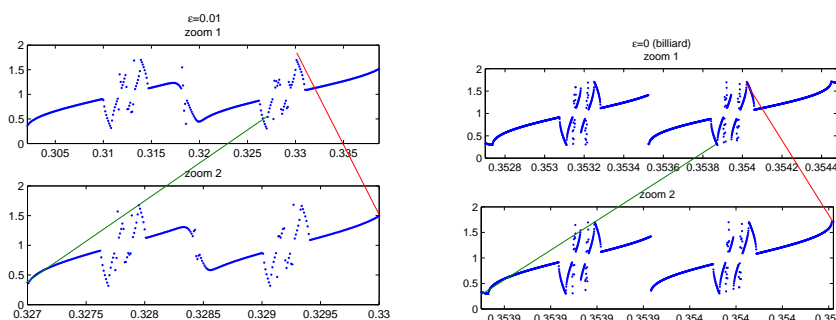


FIGURE 11. Close-up of the unresolved region of  $\Phi_2(s; \epsilon)$  near the right unresolved region for  $\epsilon = 0.01$  and billiard.

region. Furthermore, interactions between the two components of the invariant set are expected to appear, as described next.

- (3) At  $\epsilon = 0.06654$  the non-monotone behavior associated with the corner discontinuity appears to merge with the invariant set so one unresolved region disappears (Fig. 10 right). While self-similarity is still observed, its structure certainly appears to be different than the billiard scattering function. Here, we see that the bifurcations associated with the corner influence the structure of the invariant set.
- (4) For  $\epsilon = 0.1403$  (elliptic island) and  $\epsilon = 0.1146$  (period doubling) the residence time functions  $T(s; \epsilon)$  have significant peaks (see Fig. 9) that are associated with

sticky orbits. The scattering functions for these values of  $\varepsilon$  appear to have a fractal dimension close to 1: at the center of Fig. 10 we show that zooming-in in the unresolved regions produces singular curves with wide spread singularities. Both findings are typical to the scattering functions that appear when the invariant set has KAM-tori [25].

- (5) At  $\varepsilon = 0.1842$ , above the wedge of stability, the scattering is regular and resembles the case of scattering by two discs (i.e.  $n = 1$ , see Fig. 13). We propose that at this value of  $\varepsilon$  the level set near the corner is so smooth that the invariant set consists of one hyperbolic periodic orbit as in the two discs case.
- (6) For  $\varepsilon = 0.4698$  the invariant set for the energy level  $h = 1/2$  is empty and the scattering function  $\Phi(s; \varepsilon)$  is smooth.

A similar behavior is observed in the tangent geometry, as shown in Fig. 12; while increasing  $\varepsilon$  leads to the merger of unresolved intervals, the fractal dimension of the scattering function at the stability wedges appears to approach one. This behavior is not obvious from figure 12 that shows the global structure of the scattering function. Yet, zooming on the unresolved intervals produces similar behavior to the one described above, namely self similar structure which thins out as  $\varepsilon$  is increased and is away from the stability wedges, and singular structure with fractal dimension approaching one inside and close to the stability wedges.

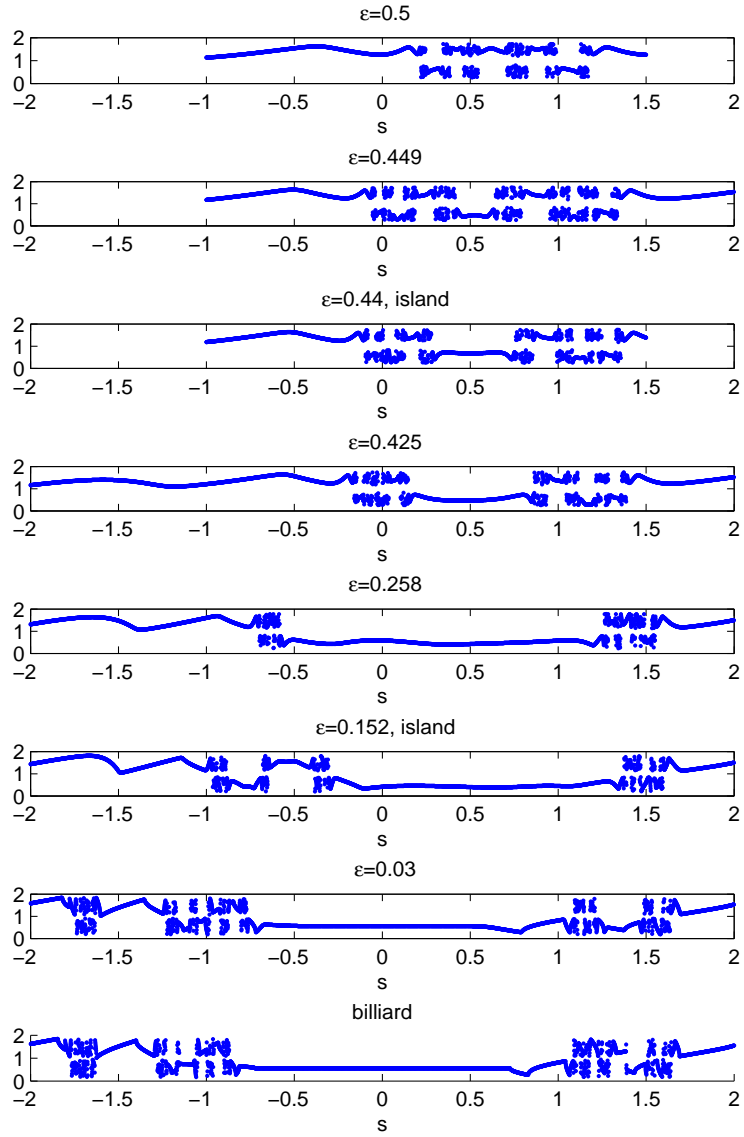
## 5. SUMMARY AND CONCLUSIONS

The fractal dimension of the scattering function of a family of two-dimensional smooth potentials depends sensitively on the order parameters, and, in general, is impossible to predict. Indeed, the structure of the invariant set, which is usually of mixed nature, undergoes many bifurcations as the parameters are varied, and thus cannot be fully characterized by finite grammar symbolic sequences that are stable under parameter variations. We show that by utilizing the singular billiard limit, the structure of the scattering function of smooth steep potentials may be controlled. More precisely, we first observed that the relation between the invariant set of the smooth flow and of the billiard flow is explained by [38][44] and [34]. Thus, we showed that when the invariant set of the billiards is uniformly hyperbolic and bounded away from singularities (e.g. in the case of regular Sinai scatterers), the scattering function of the steep smooth flow approaches that of the billiard. On the other hand, we showed that tangent periodic orbits of dispersing billiards and some of their corner polygons give rise to islands of stability in the smooth flow at wedges of parameter values that emanate from the  $\mu$ -axis. In particular, a substantial increase in the fractal dimension of the scattering function appears for arbitrary small  $\varepsilon$  values. In other words, the fractal dimension of the scattering function of the smooth flow can be controlled by tuning the ratio between the steepness parameter and the billiard geometrical parameters. The location of the wedges may be found numerically, as demonstrated here, or analytically, as in [38, 44].

To elucidate and demonstrate these findings we studied scattering by two families of singular Sinai billiards: one with four disjoint discs and one with  $n$  overlapping discs (creating  $n - 1$  corners) and additional disjoint disc. Scattering by such billiards are relatively well understood: usually<sup>17</sup>, using geometrical methods, the invariant set may be fully characterized by employing symbolic dynamics with finite number of symbols and finite grammar

---

<sup>17</sup>for almost all parameter values.

FIGURE 12. Scattering function  $\Phi(s; \epsilon)$  for the tangent case at  $\mu = 0.1$ .

(finite partition) [13, 14]. When the parameters are varied, the invariant set may undergo bifurcations, and the grammar changes at the bifurcation points. Since the invariant set is hyperbolic, a bifurcation point necessarily corresponds to the appearance of singular orbits in the invariant set. Most previous works on billiard scattering examined smooth convex (mainly circular) obstacles, so the only singularities of the invariant set that were studied were associated with tangencies. We demonstrated here that another source for such bifurcations are corners. Moreover, we showed that corners lead to discontinuous scattering functions whereas tangencies lead to continuous, non-differentiable scattering functions that are non-monotone only at the singular tangent points. For a specific geometrical set up, we found an explicit formula relating the fractal dimension of the scattering function to the number of corners of the scatterer, yet we propose that a more detailed analysis is needed. Such an analysis may result in finding the signatures of different types of corners on the scattering functions.

Studying the scattering functions of smooth steep potentials that approach singular Sinai scatterers, the following scenario emerges; Let  $\mu^*$  denote a bifurcation value for which the billiard invariant set has a singularity, so that a stability wedge in the  $(\mu, \varepsilon)$  plane emanates from  $(\mu^*, 0)$  (i.e. the smooth flow has stable periodic orbit for all parameters in this wedge) [38, 44]. For a fixed  $\mu$  value intersecting this wedge, there exist an interval of  $\varepsilon$  values,  $[\varepsilon^-(\mu), \varepsilon^+(\mu)]$ , at which the periodic orbit is stable. At one edge of this interval the periodic orbit undergoes a saddle-center bifurcation and at the other end a period doubling bifurcation. Fixing such a "generic"  $\mu$  value close to  $\mu^*$ , where at  $\mu$  the billiard invariant set is hyperbolic and non-singular, and  $\varepsilon^\pm(\mu)$  are small, the following sequence of bifurcations occurs as  $\varepsilon$  is increased from  $0^+$ :

- (1) For a sufficiently small  $\varepsilon$  the hyperbolicity is preserved so the scattering function is self-similar, and its fractal dimension approaches that of the billiard scattering function at  $\mu$ . Isolated discontinuities in the billiard scattering function may lead to additional singular components in the scattering function of the smooth flow.
- (2) Increasing  $\varepsilon$  towards and through the interval  $[\varepsilon^-(\mu), \varepsilon^+(\mu)]$  leads to a sequence of Hamiltonian bifurcations of the hyperbolic periodic orbits that produces elliptic orbits. These bifurcations appear in the scattering function as the merge between several unresolved regions. For  $\varepsilon$  values inside the wedges of stability, the signature of non-hyperbolic chaotic scattering shows up – the density of singularities is large and does not appear to converge to a discrete set as further magnifications are employed. We notice that the stability interval  $[\varepsilon^-(\mu), \varepsilon^+(\mu)]$  indicates the stability property of a single periodic orbit. At least near the period-doubling end of this interval there exist a cascade of other periodic orbits that are stable, hence, the non-hyperbolic interval is certainly larger than  $[\varepsilon^-(\mu), \varepsilon^+(\mu)]$ .
- (3) Further small increase of  $\varepsilon$  beyond the stability interval may lead to the appearance of additional interval of hyperbolic scattering or to the appearance of another interval of stability that stems from another stability wedge emanating from some other  $\mu^{**}$ . Depending on how far the stability wedges are located from each other, the scattering may be either non-hyperbolic (with some KAM-tori) or hyperbolic with a fractal dimension that is smaller than the one appearing for the billiard limit.
- (4) A larger increase in  $\varepsilon$  is problem specific and may involve some topological changes of the corresponding Hill's region. In our examples, it finally leads to the reduction of the invariant set to one unstable periodic orbit and then to the destruction of the invariant set.

The above description suggests that by choosing a one parameter family of steep potentials  $(\mu, \varepsilon(\mu)) \rightarrow (\mu^*, 0)$  such that  $\varepsilon(\mu) \in (\varepsilon^-(\mu), \varepsilon^+(\mu))$  for all  $\mu$  values (see Fig. 6), the fractal dimension of the corresponding scattering function is 1 for arbitrary small  $\varepsilon$ . While the fractal dimension of the billiard scattering is expected to be discontinuous across  $\mu^*$ , there is no evidence that it approaches one at these singular  $\mu$  values. Thus, we conjecture that the fractal dimension of the scattering function is continuous in  $\varepsilon$  at  $0^+$  for regular  $\mu$  values and is discontinuous in  $\varepsilon$  at  $0^+$  at singular  $\mu$  values.

Another interesting aspect of our results is the ability to numerically detect non-ergodic behavior in steep potentials that limit to Sinai billiards on the torus, without the need of phase space plots: embedding the torus in the plane, islands of stability are expected to cause the fractal dimension of the scattering functions to approach one. Thus, the fractal dimension of the scattering function may be used as a detection tool for locating (non accelerating) islands of stability.

Finally, we note that [34] implies that scattering by multi-dimensional smooth steep potentials may be similarly analyzed by studying scattering by the limiting multi-dimensional billiards. Moreover, we have recently shown that in such situations, for arbitrary large dimension, islands of stability may emerge [35]. The influence of such islands on the multi-dimensional scattering functions are yet to be studied. More generally, in the multi-dimensional case there are numerous types of singularities and bifurcations, and their expression in the scattering functions are yet to be found. The proposed methodology may be useful in exploring these issues.

**Acknowledgement 1.** *We thank Uzy Smilansky and Dmitry Turaev for stimulating discussions and important comments. We acknowledge support by the Israel Science Foundation (Grant 926/04) and by a joint grant from the Ministry of Science, Culture and Sport, Israel and the Russian Foundation for basic research, the Russian Federation.*

#### APPENDIX A. CLOSENESS THEORY

Let us first recall the conditions  $W(q; \varepsilon)$  needs to satisfy so that the regular trajectories of the billiard will be shadowed by trajectories of the smooth flow [35] in  $\mathcal{D} = S_{R+\Delta}^{interior} \setminus D$  (taking a fixed  $\Delta > 0$  insures that the section  $q \in S_R$  consists of interior points of the billiard flow in  $\mathcal{D}$ ):

**Condition I.** *For any fixed (independent of  $\varepsilon$ )  $R$  and a compact region  $K \subset \mathcal{D}$  the potential  $W(q; \varepsilon)$  diminishes along with all its derivatives as  $\varepsilon \rightarrow 0$ :*

$$(22) \quad \lim_{\varepsilon \rightarrow 0} \|W(q; \varepsilon)|_{q \in K}\|_{C^{r+1}} = 0.$$

The growth of the potential near the boundary for sufficiently small  $\varepsilon$  values is treated as in [38]. We assume that the level sets of  $W$  may be realized by some *finite* function near the boundary. Namely, let  $N(\Gamma^*)$  denote the fixed (independent of  $\varepsilon$ ) neighborhood of the corner set and  $N(\Gamma_i)$  denote the fixed neighborhood of the smooth boundary component  $\Gamma_i$ ; define  $\tilde{N}_i = N(\Gamma_i) \setminus N(\Gamma^*)$  (we assume that  $\tilde{N}_i \cap \tilde{N}_j = \emptyset$  when  $i \neq j$ ). Assume that for all small  $\varepsilon \geq 0$  there exists a *pattern function*

$$Q(q; \varepsilon) : \bigcup_i \tilde{N}_i \rightarrow \mathbb{R}^1$$

which is  $C^{r+1}$  with respect to  $q$  in each of the neighborhoods  $\tilde{N}_i$  and it depends continuously on  $\varepsilon$  (in the  $C^{r+1}$ -topology, so it has, along with all derivatives, a proper limit as  $\varepsilon \rightarrow 0$ ). Further assume that in each of the neighborhoods  $\tilde{N}_i$  the following is fulfilled.

**Condition IIa.** *The billiard boundary is composed of level surfaces of  $Q(q; 0)$ <sup>18</sup>:*

$$(23) \quad Q(q; \varepsilon = 0)|_{q \in \Gamma_i \cap \tilde{N}_i} \equiv Q_i = \text{constant.}$$

In the neighborhood  $\tilde{N}_i$  of the boundary component  $\Gamma_i$  (so  $Q(q; \varepsilon)$  is close to  $Q_i$ ), define a barrier function  $\mathcal{W}_i(Q; \varepsilon)$ , which is  $C^{r+1}$  in  $Q$ , continuous in  $\varepsilon$  and does not depend explicitly on  $q$ , and assume that there exists  $\varepsilon_0$  such that

**Condition IIb.** *For all  $\varepsilon \in (0, \varepsilon_0]$  the potential level sets in  $\tilde{N}_i$  are identical to the pattern function level sets and thus:*

$$(24) \quad W(q; \varepsilon)|_{q \in \tilde{N}_i} \equiv \mathcal{W}_i(Q(q; \varepsilon) - Q_i; \varepsilon),$$

and

**Condition IIc.** *For all  $\varepsilon \in (0, \varepsilon_0]$ ,  $\nabla W$  does not vanish in the finite neighborhoods of the boundary surfaces,  $\tilde{N}_i$ , thus:*

$$(25) \quad \nabla Q|_{q \in \tilde{N}_i} \neq 0$$

and for all  $Q(q; \varepsilon)|_{q \in \tilde{N}_i}$

$$(26) \quad \frac{d}{dQ} \mathcal{W}_i(Q - Q_i; \varepsilon) \neq 0.$$

Now, the rapid growth of the potential across the boundary may be described in terms of the barrier functions alone. Note that by (25), the pattern function  $Q$  is monotone across  $\Gamma_i \cap \tilde{N}_i$ , so either  $Q > Q_i$  corresponds to the points near  $\Gamma_i$  inside  $K$  and  $Q < Q_i$  corresponds to the outside, or vice versa. To fix the notation, we will adopt the first convention.

**Condition III.** *There exists a constant (may be infinite)  $\mathcal{E}_i > 0$  such that as  $\varepsilon \rightarrow +0$  the barrier function increases from zero to  $\mathcal{E}_i$  across the boundary  $\Gamma_i$ :*

$$(27) \quad \lim_{\varepsilon \rightarrow +0} \mathcal{W}(Q; \varepsilon) = \begin{cases} 0, & Q > Q_i \\ \mathcal{E}_i, & Q < Q_i \end{cases}.$$

Let,

$$(28) \quad \mathcal{E} = \min_{i=1, \dots, \bar{n}} \mathcal{E}_i.$$

By (26), for small  $\varepsilon$ ,  $Q$  could be considered as a function of  $\mathcal{W}$  and  $\varepsilon$  near the boundary:  $Q = Q_i + Q_i(\mathcal{W}; \varepsilon)$ . Condition IV states that for small  $\varepsilon$  a finite change in  $\mathcal{W}$  corresponds to a small change in  $Q$ :

**Condition IV.** *As  $\varepsilon \rightarrow +0$ , for any fixed  $\mathcal{W}_1$  and  $\mathcal{W}_2$  such that  $0 < \mathcal{W}_1 < \mathcal{W}_2 < \mathcal{E}$ , for each boundary component  $\Gamma_i$ , the function  $Q_i(\mathcal{W}; \varepsilon)$  tends to zero uniformly on the interval  $[\mathcal{W}_1, \mathcal{W}_2]$  along with all its  $(r+1)$  derivatives.*

In [34] it was shown that not only can we establish that the regular hyperbolic orbits of the billiard flow and the smooth flow are close, we can even find the order of the correction terms. To this aim, following [34], we define the bounds on the rate at which  $\mathcal{W}(Q)$  (respectively  $Q(\mathcal{W})$ ) approach zero as the exterior part of the boundary layer (respectively the interior part of the boundary layer) is approached. First we define the region  $\mathcal{D}_{in}^\varepsilon$ ; Choose some  $\delta(\varepsilon) \rightarrow +0$  such that for every boundary surface  $\Gamma_i$ , the surfaces

<sup>18</sup>This is the  $Q(x, y; 0)$  defined in Section 2.1.

$Q(q; \varepsilon)|_{q \in \tilde{N}_i} = Q_i + \delta(\varepsilon)$  together with  $\partial N(\Gamma^*)$  bound a region  $\mathcal{D}_{int}^\varepsilon$  inside  $\mathcal{D}$  in which the potential  $W$  tends to zero uniformly along with all its derivatives. Let

$$(29) \quad m^{(r)}(\delta; \varepsilon) = \sup_{\substack{q \in \mathcal{D}_{int}^\varepsilon \\ 1 \leq l \leq r+1}} \|\partial^l V(q; \varepsilon)\|.$$

According to Conditions I and III,  $m^{(r)}$  approaches zero as  $\varepsilon \rightarrow 0$  for any fixed  $\delta > 0$ , therefore the same holds true for any choice of sufficiently slowly tending to zero  $\delta(\varepsilon)$ .

We then define the auxiliary billiard domain  $\mathcal{D}^\varepsilon$ : for each  $i$ , take any  $v_i(\varepsilon) \rightarrow +0$  such that the function (inverse barrier)  $Q_i(\mathcal{W}; \varepsilon)$  tends to zero along with all its derivatives, uniformly for  $h \geq \mathcal{W} \geq v_i$  (recall that  $h < \mathcal{E}_i$  for all  $i$ ). We will use the notation

$$(30) \quad M_i^{(r)}(v_i; \varepsilon) = \sup_{\substack{v_i \leq W \leq h \\ 0 \leq l \leq r+1}} |Q_i^{(l)}(W; \varepsilon)|.$$

Condition IV implies that  $M^{(r)}$  (the vector of all  $M_i^{(r)}(v_i; \varepsilon)$ ) approaches zero as  $\varepsilon \rightarrow 0$  for any fixed vector of  $v(\varepsilon)$  with  $v_i > 0$ , hence the same holds true for any sufficiently slowly tending to zero  $v(\varepsilon)$ , i.e. the required  $v_i(\varepsilon)$  exist. Let  $\eta_i(\varepsilon) = Q_i(v_i; \varepsilon)$  and consider the billiard in the domain  $\mathcal{D}^\varepsilon$  which is bounded by the surfaces  $\Gamma_i^\varepsilon : Q(q; \varepsilon)|_{q \in \tilde{N}_i} = Q_i + \eta_i(\varepsilon)$ . For sufficiently small  $\varepsilon$ , the surface  $\Gamma_i^\varepsilon$  is a smooth surface which is close to  $\Gamma_i$  and is completely contained in  $\tilde{N}_i$  (its boundaries belong to  $N(\Gamma^*)$ ). Indeed, recall that the boundaries  $\Gamma_i$  of the original scatterer  $\mathcal{D}$  are given by the level sets  $Q(q; 0) = Q_i$  and that  $\eta_i(\varepsilon)$  is small, so the new billiard is close to the original one. In particular, for regular reflections, the billiard map  $B^\varepsilon$  of the auxiliary billiard defined in  $\mathcal{D}^\varepsilon$  tends to the original billiard map  $B$  along with all its derivatives. It is easy to see that for  $\varepsilon > 0$ , the domains thus obtained obey  $\mathcal{D}_{int}^\varepsilon \subset \mathcal{D}^\varepsilon \subset \mathcal{D}_{Hill}(h) \subset \mathcal{D}$ , where  $\mathcal{D}_{Hill}$  denotes the Hill's region, the region exterior to the level sets  $W(q; \varepsilon) = h$  that surround the scatterers for sufficiently small  $\varepsilon$ .

In [34] it was established that the auxiliary billiard map,  $B^\varepsilon$ , defined by the region  $\mathcal{D}^\varepsilon$ , provides an excellent approximation to the smooth flow as long as singularities (tangencies and corners) are avoided: away from a small boundary layer which can be precisely estimated, it is close, together with its  $r$  derivatives to the smooth flow and it may be used to find the next order correction terms. Moreover, it was established that a global Poincaré map  $\Phi^\varepsilon$  of the smooth flow may be defined on the cross-section

$$(31) \quad S_\varepsilon = \{\rho = (q, p) : q \in \partial \mathcal{D}^\varepsilon, \langle p, n(q) \rangle > 0\}$$

for regular orbits - orbits that intersect  $\partial \mathcal{D}^\varepsilon$  at an angle bounded away from zero, and that this map is  $C^r$ -close to the auxiliary billiard map  $B^\varepsilon$ . As the billiard map  $B^\varepsilon$  is close to the original billiard map  $B$ , we obtain the closeness of the Poincaré map  $\Phi^\varepsilon$  to  $B$  as well<sup>19</sup>. The following theorem, follows directly from [34]:

**Theorem 2.** *Consider a Hamiltonian system with a potential  $W(q, \varepsilon)$  satisfying Condition I-IV in the domain  $\mathcal{D} = S_R^{interior} \setminus D$ , where  $D$  is a Sinai scatterer. Choose  $v(\varepsilon), \delta(\varepsilon)$  such that  $v(\varepsilon), \delta(\varepsilon), m^{(1)}(\varepsilon), M^{(1)}(\varepsilon) \rightarrow 0$  as  $\varepsilon \rightarrow 0$ . Let  $P^b(t)$  denote a regular hyperbolic orbit for the billiard flow in  $\mathcal{D}$ . Then, for any  $h \in (0, \mathcal{E})$ , for sufficiently small  $\varepsilon$ , the smooth Hamiltonian flow has a uniquely defined hyperbolic orbit  $P^\varepsilon(t)$  which stays  $O(v + m^{(1)} + M^{(1)})$ -close to  $P^b(t)$  for all  $t$  outside of the collision intervals (finitely many of them in*

<sup>19</sup>In [34], the map  $B^\varepsilon$  (rather than  $B$ ) is used as the zeroth order approximation for an explicit asymptotic expansions for  $\Phi^\varepsilon$ .

any finite interval of time) of length  $O(|\delta| + M^{(1)})$ . Away from the collision intervals, the local Poincaré map near  $P^\varepsilon$  is  $O_{C^r}(\nu + m^{(r)} + M^{(r)})$ -close to the local Poincaré map near  $P^b(t)$ . In particular, the stable and unstable manifolds of  $P^\varepsilon$  approximate  $O_{C^r}(\nu + m^{(r)} + M^{(r)})$ -closely the stable and unstable manifolds of  $P^b(t)$  on any compact, forward-invariant or, respectively, backward-invariant piece bounded away from the singularity set in the billiard's phase space.

*Proof.* See theorem 5 of [34] where this theorem is proved for periodic orbits. Here we simply use the note of [34] that the same results and proof apply to any regular hyperbolic orbit, with the same error estimates as for the hyperbolic periodic orbit case. By regular hyperbolic orbit, we mean that this orbit is bounded away from the singularity set.  $\square$

Table 3.3.1 in [34] supplies the optimized error estimates and the boundary layer scalings for typical potentials (power-laws, exponentials and Gaussian). For example, for the exponential potential which is used here we find that by choosing a boundary layer width of order  $O(\varepsilon |\ln \varepsilon|)$  the auxiliary billiard regular trajectories are  $O_{C^r}(\varepsilon^{r+2})$  close to the corresponding smooth flow trajectories. Using the existence of a Poincaré map  $\Phi^\varepsilon$  that is close to the billiard map away from tangent reflections, it is easy to establish that regular hyperbolic sets appear also for the smooth flow as stated in corollary 1. Indeed, consider the billiard partition which is used to construct  $\Lambda$ . By assumption on the regularity of  $D$ , each component is mapped to its image by a regular reflection (namely, there are no tangent reflections). It follows that for sufficiently small  $\varepsilon$ , the image of the partition components under the Poincaré map  $\Phi^\varepsilon$ , which is well defined for all orbits in these components since they all have non-tangent reflections, is close, in the  $C^r$  topology, to the image of the components under the auxiliary billiard map (i.e. both the topology of the invariant set and the hyperbolicity properties that are governed by the first derivatives of the billiard map are inherited by the Poincaré map of the smooth flow). It follows that the invariant sets of  $\Lambda$  and  $\Lambda^\varepsilon$  are conjugated by the same symbolic dynamics and that their Lyapunov exponents and cone structure are  $C^r$  close as well.

Let us now examine how these results translate to the properties of the scattering map:

**Corollary 2.** *Under the same conditions of theorem 2, if  $(s_{in}(b_{in}, \varphi_{in}; R), \varphi_{in})$  is a non-trivial regular value (respectively,  $(s_{in}, \varphi_{in}) \in \Sigma_{tan}$  has a finite number of collisions, one tangent and all the rest regular) of the billiard scattering map  $S$ , then there exists a nearby initial condition  $(s_{in}^\varepsilon, \varphi_{in}^\varepsilon)$ , limiting to  $(s_{in}, \varphi_{in})$  as  $\varepsilon \rightarrow 0$ , such that the smooth scattering map  $S^\varepsilon$  is  $C^r$  close (respectively, is  $C^0$  close) to  $S$  at  $(s_{in}, \varphi_{in})$ . Furthermore, for the regular case, away from the short collision intervals of length  $O(|\delta| + M^{(1)})$ , the orbit of  $(s_{in}^\varepsilon, \varphi_{in}^\varepsilon)$  is  $O(\nu + m^{(1)} + M^{(1)})$ -close to the corresponding orbit of the billiard flow.*

*Proof.* Recall that the scatterers are assumed to be dispersing so if  $(s_{in}, \varphi_{in})$  is a regular orbit it is necessarily hyperbolic.  $\square$

Fig. 13, in which only two circular obstacles are considered (as in [11]), demonstrates these closeness results. In this case the invariant set has only one periodic orbit which is hyperbolic for all  $\varepsilon$  values, so the scattering is regular, and the smooth scattering function  $\Phi_1(s; \varepsilon)$  limits to  $\Phi_1(s; \varepsilon = 0)$  smoothly on its smooth parts and continuously at its singularity points. Figs. 12 and 3 demonstrate these results for sufficiently small  $\varepsilon$  (non-uniformly in the distance from the singular Sinai scatterers).

Finally, we note that we did not analyze the far field behavior of the scattering functions, behavior which depends on the rate of decay of the potential. In principle, to obtain similar results uniformly in  $R$ , so that impact coordinates may be used in the smooth case, one

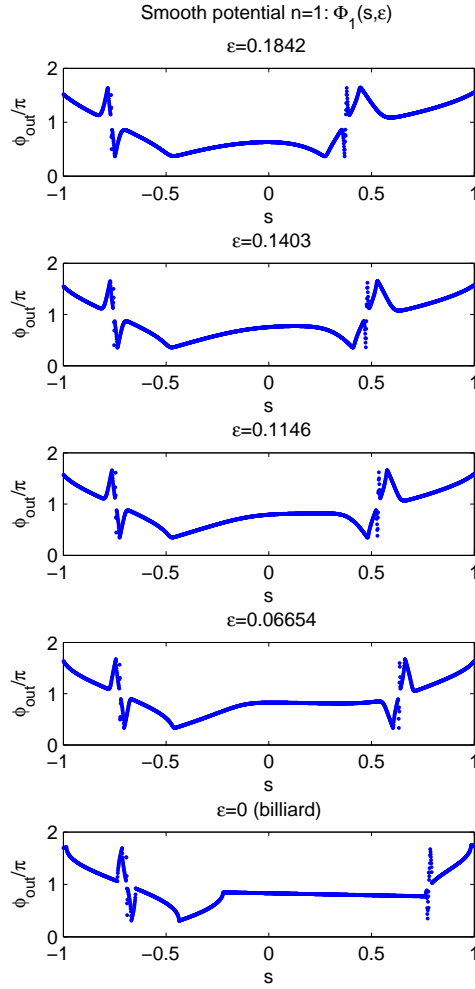


FIGURE 13. Scattering function for a simple invariant set - one hyperbolic orbit ( $\Phi_1(s; \epsilon)$ ) for the case of two disks, i.e.  $n = 1$ .

needs to impose sufficiently rapid decay rate of the potential at large  $q$  values. We propose that imposing the following condition should suffice:

**Condition V.** *There exists an  $R$ , such that for all  $|q| \geq R$ , there exists  $\alpha > 0$  ( $R$  and  $\alpha$  are independent of  $\epsilon$ ) and a function  $A(\epsilon)$  which limits to 0 as  $\epsilon \rightarrow 0$ , such that for all  $\epsilon \in (0, \epsilon_{\max})$*

$$(32) \quad |W(q; \epsilon)| \leq \frac{A(\epsilon)}{|q|^\alpha},$$

*in the  $C^{r+1}$  topology.*

Indeed, using this condition, it is easy to show by successive approximation method of the integral form of the Hamiltonian flow (1) that the asymptotic velocities  $(p_x^\varepsilon(\pm\infty), p_y^\varepsilon(\pm\infty))$  and thus the corresponding asymptotic directions  $\varphi_{in,out}^\varepsilon$  may be defined on  $S_R$  (see, e.g. [44]). While (32) is not sufficient to guarantee that an asymptotic direction  $s_{in}$  exists, it is still possible to define asymptotic impact parameter  $\eta_{in}$  as in [44]. Then the mapping from  $S(R_\infty)$  where  $R_\infty \gg R$  to  $S(R)$  is smooth and the properties of the smooth scattering map at  $S(R)$  are inherited by the smooth scattering map at  $S(R_\infty)$ .

## REFERENCES

- [1] H. Aref, *Stirring by chaotic advection*, J. Fluid Mech. **192** (1984), 115–173.
- [2] S. Bleher, C. Grebogi, E. Ott, and R. Brown, *Fractal boundaries for exit in hamiltonian dynamics*, Phys. Rev. A **38** (1988), 930–938.
- [3] S. Bleher, E. Ott, and C. Grebogi, *Routes to chaotic scattering*, Phys. Rev. Lett. **63** (1989), no. 9, 919–922.
- [4] Siegfried Bleher, Celso Grebogi, and Edward Ott, *Bifurcation to chaotic scattering*, Phys. D **46** (1990), no. 1, 87–121.
- [5] P. T. Boyd and S. L. W. McMillan, *Chaotic scattering in the gravitational three-body problem*, Chaos: An Interdisciplinary Journal of Nonlinear Science **3** (1993), no. 4, 507–523.
- [6] W. Breymann, Z. Kovács, and T. Tél, *Chaotic scattering in the presence of an external magnetic field*, Phys. Rev. E **50** (1994), 1994–2006.
- [7] Y-C. Chen, *Anti-integrability in scattering billiards*, Dyn. Syst. **19** (2004), no. 2, 145–159.
- [8] A. A. Chernikov and G. Schmidt, *Chaotic scattering and acceleration of particles by waves*, Chaos: An Interdisciplinary Journal of Nonlinear Science **3** (1993), no. 4, 525–528.
- [9] Vincent Daniels, Michel Vallieres, and Jian-Min Yuan, *Chaotic scattering on a double well: Periodic orbits, symbolic dynamics, and scaling*, Chaos: An Interdisciplinary Journal of Nonlinear Science **3** (1993), no. 4, 475–485.
- [10] ———, *Chaotic scattering on a billiard*, Phys. Rev. E **57** (1997), no. 2, 1519–1531.
- [11] M. Ding, C. Grebogi, E. Ott, and J. A. Yorke, *Transition to chaotic scattering*, Phys.Rev.A **42** (1990), 7025–7040.
- [12] J. R. Dorfman and P. Gaspard, *Chaotic scattering theory of transport and reaction-rate coefficients*, Phys. Rev. E **51** (1995), no. 1, 28–35.
- [13] B. Eckhardt, *Fractal properties of scattering singularities*, Journal of Physics A: Mathematical and General **20** (1987), no. 17, 5971–5979.
- [14] P. Gaspard and S.A. Rice, *Scattering from a classically chaotic repeller*, J. Chem. Phys. **90** (1989), no. 4, 2225–2241.
- [15] Kai T. Hansen and Achim Kohler, *Chaotic scattering through potentials with rainbow singularities*, Phys. Rev. E **54** (1996), no. 6, 6214–6225.
- [16] M. Hénon, *Chaotic scattering modelled by an inclined billiard*, Phys. D **33** (1988), no. 1-3, 132–156.
- [17] Jarmo Hietarinta and Seppo Mikkola, *Chaos in the one-dimensional gravitational three-body problem*, Chaos: An Interdisciplinary Journal of Nonlinear Science **3** (1993), no. 2, 183–203.
- [18] Moser J.K. and P. J. Holmes, *Stable and random motions in dynamical systems: With special emphasis on celestial mechanics*, Princeton University Press, 2001.
- [19] C. Jung and H. J. Scholz, *Cantor set structures in the singularities of classical potential scattering*, Jour. of Phys. A **20** (1987), 3607–3617.
- [20] C. Jung and T. H. Seligman, *Integrability of the s-matrix versus integrability of the hamiltonian*, Phys. Rep. **285** (1997), 77–141.
- [21] M. Klein and A. Knauf, *Classical planar scattering by coulombic potentials*, Springer-Verlag, New York, 1992.
- [22] A. Knauf, *The n-centre problem of celestial mechanics for large energies*, Journal of the European Mathematical Society **4** (2002), no. 1, 1–114.
- [23] A. Knauf and I.A. Taimanov, *On the integrability of the n-centre problem*, Mathematische Annalen **331** (2005), no. 3, 631–649.
- [24] B.-P. Koch and B. Bruhn, *Phase space structure and chaotic scattering in near-integrable systems*, Chaos: An Interdisciplinary Journal of Nonlinear Science **3** (1993), no. 4, 443–457.
- [25] Y.T. Lau, J.M. Finn, and E. Ott, *Fractal dimension in nonhyperbolic chaotic scattering*, Phys.Rev.Lett. **66** (1991).

- [26] K. R. Meyer and R. G. Hall, *Introduction to hamiltonian dynamical systems and the n-body problem*, Applied Mathematical Sciences, vol. 90, Springer-Verlag, NY, 1991.
- [27] D. W. Noid, Stephen K. Gray, and Stuart A. Rice, *Fractal behavior in classical collisional energy transfer*, The Journal of Chemical Physics **84** (1986), no. 5, 2649–2652.
- [28] E. A. Novikov and I. B. Sedov, *Vortex collapse*, Zhurnal Eksperimental noi i Teoreticheskoi Fiziki **77** (1979), 588–597.
- [29] E. Ott and T. Tel, *Chaotic scattering: An introduction*, Chaos **3** (1993), no. 4, 417–426.
- [30] Edward Ott, *Chaos in dynamical systems*, second ed., Cambridge University Press, Cambridge, 2002.
- [31] J.-M. Petit and M. Henon, *A numerical simulation of planetary rings. II - Monte Carlo model*, Astronomy and Astrophysics **188** (1987), 198–205.
- [32] C. C. Rankin and W. H. Miller, *Classical s matrix for linear reactive collisions of  $h + cl$  [sub 2]*, The Journal of Chemical Physics **55** (1971), no. 7, 3150–3156.
- [33] A. Rapoport and V. Rom-Kedar, *Nonergodicity of the motion in three-dimensional steep repelling dispersing potentials*, Chaos **16** (2006), no. 4, 043108.
- [34] A. Rapoport, V. Rom-Kedar, and D. Turaev, *Approximating multi-dimensional Hamiltonian flows by billiards*, to appear in CMP (2006).
- [35] A. Rapoport, V. Rom-Kedar, and D. Turaev, *High dimensional linearly stable orbits in steep, smooth, strictly dispersing billiard potentials*, preprint (2007).
- [36] S. Ree and L. E. Reichl, *Fractal analysis of chaotic classical scattering in a cut-circle billiard with two openings*, Phys. Rev. E **65** (2002), no. 5, 055205.
- [37] V. Rom-Kedar, A. Leonard, and S. Wiggins, *An analytical study of transport, mixing and chaos in an unsteady vortical flow*, J. Fluid Mech. **214** (1990), 347–394.
- [38] V. Rom-Kedar and D. Turaev, *Big islands in dispersing billiard-like potentials*, Physica D **130** (1999), 187–210.
- [39] L. P. Shilnikov and D. V. Turaev, *Super-homoclinic orbits and multi-pulse homoclinic loops in Hamiltonian systems with discrete symmetries*, Regul. Khaoticheskaya Din. **2** (1997), no. 3-4, 126–138, V. I. Arnold (on the occasion of his 60th birthday) (Russian).
- [40] Ya.G. Sinai, *Dynamical systems with elastic reflections: Ergodic properties of scattering billiards*, Russian Math. Sur. **25** (1970), no. 1, 137–189.
- [41] T. Tel, C. Grebogi, and E. Ott, *Conditions for the abrupt bifurcation to chaotic scattering*, Chaos **3** (1993), no. 4, 495–503.
- [42] G. Troll and U. Smilansky, *A simple model for chaotic scattering i. classical theory.*, Physica D (1989), no. 35, 34–64.
- [43] D. Turaev and V. Rom-Kedar, *Islands appearing in near-ergodic flows*, Nonlinearity **11** (1998), no. 3, 575–600.
- [44] D. Turaev and V. Rom-Kedar, *Soft billiards with corners*, J. Stat. Phys. **112** (2003), no. 3–4, 765–813.
- [45] D. V. Turaev and L. P. Shilnikov, *Hamiltonian systems with homoclinic saddle curves*, Dokl. Akad. Nauk SSSR **304** (1989), no. 4, 811–814.
- [46] D. Wintgen, K. Richter, and G. Tanner, *The semiclassical helium atom*, Chaos: An Interdisciplinary Journal of Nonlinear Science **2** (1992), no. 1, 19–33.
- [47] Jian-Min Yuan and Yan Gu, *Chaotic electronic scattering with  $he^{sup + J}$* , Chaos: An Interdisciplinary Journal of Nonlinear Science **3** (1993), no. 4, 569–580.

ANNA.RAPOPORT@WEIZMANN.AC.IL, VERED.ROM-KEDAR@WEIZMANN.AC.IL, WEIZMANN INSTITUTE, REHOVOT, ISRAEL.